Chapter 5

Analysis of Fatty Acids by APCI-MS

Tomáš Řezanka and Jaroslav Votruba

Institute of Microbiology, Videnska 1083, 14220 Prague, Czech Republic

Introduction

The integration of chromatographic and spectroscopic analytical techniques now represents the mainstream in advanced analysis of natural compounds. Usually, this approach can be described as a two-step procedure. In the first step, the mixture of compounds is separated by a suitable technique such as gas chromatography (GC) or high-performance liquid chromatography (HPLC). Second, a specific detection method, for example, mass spectrometry (MS), is used to obtain structural information about individual substances. In an ideal case, this approach makes it possible to identify simultaneously the individual compounds in the sample, or at least estimate their chemical structures.

A combination of GC and MS techniques is currently widely used. This approach links together in one measurement the separation, with high efficiency, of individual chemical species by GC, plus the identification of their chemical structures. However, the GC-MS technique is limited to the identification of volatile compounds. In the case of poorly volatile compounds, chemical derivatization of the sample must be performed before using GC-MS. The inherent limitation of direct measurement by the volatility, as well as the thermal degradation of labile compounds, stimulated research into a more sophisticated combination of techniques, that is, LC-MS, but the two techniques show low compatibility. In general, MS operates at a high vacuum in the range of 10^{-3} to 10^{-5} Pa, whereas the output from HPLC is a liquid phase with a flow rate between 0.5 and 2 mL/min at atmospheric pressure. The feasibility of LC-MS coupling thus depends on the fast and efficient evaporation of the liquid phase from HPLC and reduction of superfluous mobile phase in the input flow to the mass spectrometer. Various devices have been designed for this purpose.

Materials and Methods

Atmospheric Pressure Chemical Ionization

Recently, new "soft" ionization techniques such as electrospray ionization (ESI) and atmospheric pressure chemical ionization (APCI) were developed to integrate HPLC

with MS. The application of these techniques permits us to evaluate the molecular masses of detected compounds. However, the use of these methods can pose problems in determining chemical structures, because of the relatively small amount of fragments formed. If necessary, this disadvantage can be overcome by the use of tandem MS (LC-MS/MS).

APCI is a method that makes it possible to produce ions by means of a gas discharge electrode. The electrode is installed near the end of an HPLC capillary that is equipped with a pneumatic sprayer located in a small heated chamber. In this way, the liquid mobile phase can be evaporated and preheated to a very high temperature of a few hundred degrees. The high voltage on the discharge electrode produces a corona arc that ionizes the molecules of evaporated mobile phase, which are in excess when compared with the analyte. Subsequently, the ions formed from the mobile phase ionize the molecules of the analyte in the same way as in the classical chemical ionization.

APCI, when used in LC-MS, permits the use of water and organic mobile phases at flow rates of up to 2 mL/min. Such performance permits the use of both conventional and micro columns with normal or reversed phases. However, the method has some limits when applied to the analysis of fatty acid (FA); for example, the mobile phase must contain volatile electrolytes such as formic or trifluoroacetic acids or ammonium acetate.

Determination of the molecular mass by APCI-MS is based either on the presence of the protonated molecule, $[M+H]^+$, or on the existence of molecular adducts with sodium, $[M+Na]^+$, or potassium ions, $[M+K]^+$, when positive ions are detected. When negative ions are detected, the molecular mass determination can be based on the occurrence of the deprotonated molecule ions $[M–H]^-$. Occasionally, one can observe the existence of ions of adducts with very different intensities that originate from the solvents of the mobile phase, such as $[M+H+MeOH]^+$ or $[M+H+ACN]^+$.

Generally, a higher voltage applied to the inlet capillary gives rise to a higher degree of fragmentation of analyte molecules. The proper interpretation of the fragmentation patterns in APCI-MS mass spectra provides information on the chemical structures of unknown compounds, or confirms the presence of a target compound. The APCI-MS technique can be employed in the analysis of a wide spectrum of compounds in the whole polarity range from nonpolar compounds to compounds that exhibit an ionic character.

Results and Discussion

Several articles concerning APCI applications in LC-MS have been published recently. The technique is becoming widely used for the analysis of lipids and their derivatives. As shown in other chapters of this book, the LC-MS technique was successfully used in analytical systems with reversed phases (RP) for the analysis of miscellaneous natural lipid products.

FA were one of the first classes of natural products to be analyzed using GC-MS. The use of LC-MS has opened new possibilities in analyzing complex mixtures of compounds that are commonly found in biological samples. One of the most exciting advantages that LC-MS has over GC-MS is that LC-MS permits the separation and structural elucidation of compounds without purification or derivatization steps, and it also permits the identification of nonvolatile and thermally labile substances. Several ionization and detection modes, including ESI or APCI, can be used for FA analysis by LC-MS. The major advantages of LC/APCI-MS analysis of FA are the fast separation and identification of FA in natural samples, the use of high flow rates (0.1–2.0 mL/min), and that it is not necessary to derivatize the FA. Using APCI, ions can be monitored in negative or positive modes, with AcOH, HCOOH, or $AcONH_4$ being usually added to the mobile phase to facilitate FA ionization. In LC-MS analysis of FA using APCI ionization mode, one of the main factors that affects the generation of ions is the orifice voltage (see the examples herein). Further possible uses of APCI include MS-MS analysis, in which a precursor ion is mass-selected by a first mass analyzer, focused into a collision region, and then the fragments are analyzed in the second mass analyzer. This provides a more specific detection of FA and their derivatives, which makes it possible to determine the double-bond positions or branched points in the FA chains.

Surprisingly, Murphy and colleagues (1) in their extensive review mentioned only one application of the LC/APCI-MS technique for detection of FA derivatives, that is, eicosanoids in biological extracts.

APCI-MS of FAME

The APCI-MS mass spectra of FA are relatively simple and typically show a protonated molecule, $[M+H]^+$, the adduct, and some fragments that make it possible to conclusively identify positional isomers, but not double-bond positions.

FA with unusually long chain lengths and higher numbers of double bonds in the chain are extremely sensitive to thermal degradation. The GC-MS method allows the analysis of very-long-chain polyunsaturated FA up to 30:7, whereas the identification of longer chain acids has not been possible (2).

Typical fatty acid methyl esters (FAME) containing from 16 to 22 carbon atoms have been analyzed by means of LC/APCI-MS (3). The effects of orifice voltage and the total number of carbon atoms versus the number of double bonds in each homolog on mass spectra were discussed and the correction coefficients for FA homologs from saturated to hexaenoic were also mentioned.

Although it is commonly accepted that APCI gives very little fragmentation, it was possible to obtain very fragment-rich spectra by changing the cone voltage (see Fig. 5.1). At low collision energy (5 eV), the positive-ion APCI-MS mass spectrum of eicosatrienoic acid methyl ester shows the $[M+H]^+$ ion at m/z 321 as practically the only peak. Already at a moderate collision energy (50 eV), where most sample ions would survive, the $[M+H]^+$ ion is converted into fragments:

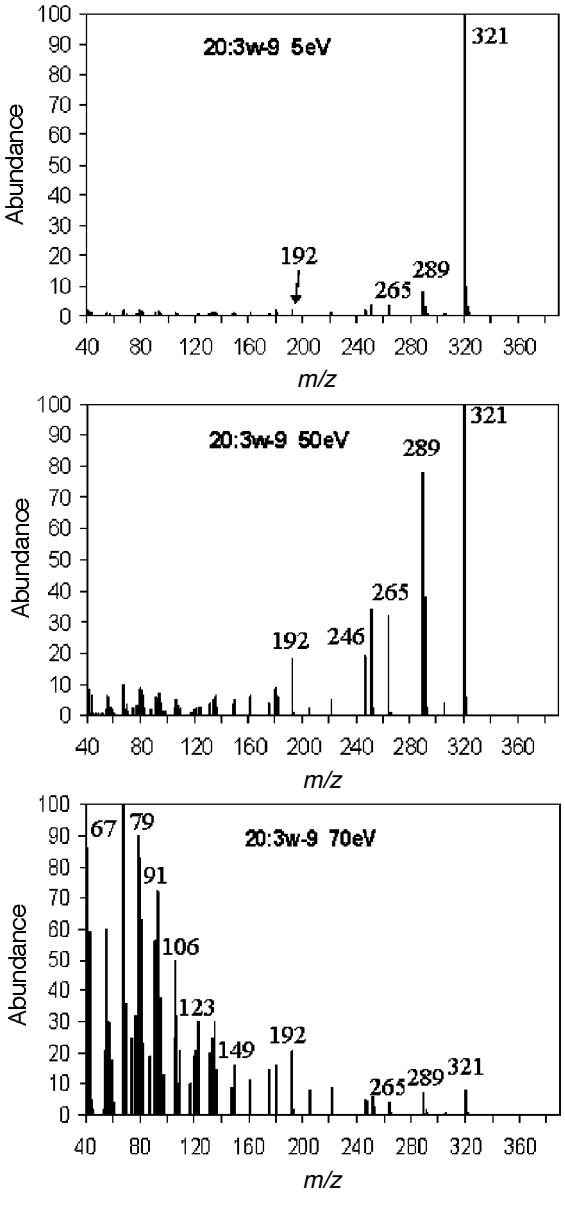

Fig. 5.1. The APCI-MS mass spectra of 20:3ω-9 methyl esters at different cone voltages.

$[M–29]^+$ or $[M–C_2H_5]^+$, $[M–31]^+$ or $[M–MeO]^+$, $[M–56]^+$ or $[M–C_4H_8]^+$, and $[M–69]^+$ or $[M–C_5H_9]^+$, at *m/z* 292, *m/z* 289, *m/z* 265, and *m/z* 252, respectively. At the highest collision energy (70 eV), the largest number of fragments are observed, especially peaks in the low region of *m/z*, that is, at *m/z* 67, 79, 93, 95, 108, 121, and so on.

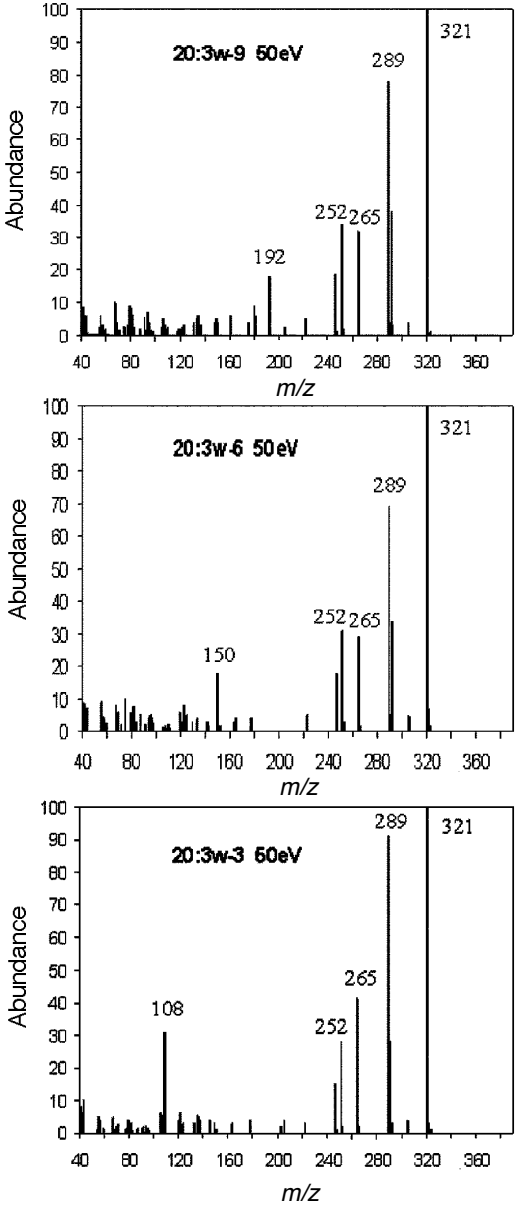

Fig. 5.2. APCI-MS mass spectra of positional isomers of eicosatrienoic fatty acid methyl esters at 50 eV.

Figure 5.2 shows mass spectra recorded at 50 eV of all three commercially available methyl esters of eicosatrienoic acid. On the basis of the well-known rule that methyl esters of several different fatty acids of the ω-3 family give a characteristic fragment at *m/z* 108 whereas those of the ω-6 series give a prominent ion at *m/z* 150

and the ω-9 family would therefore be expected to have an abundant ion at *m/z* 192, we were able to determine the positions of double bonds in methyl esters of polyunsaturated fatty acids (PUFA) from the abundances of mentioned ions in their APCI mass spectra.

The theoretical aspects of optimal performance of a suitable interface and selection of appropriate limiting parameters for interfacing supercritical fluid chromatography with MS were presented in the study by Sjoberg and Markides (4). The effects of different instrumental and chemical parameters were investigated to optimize the ion current signal and stability of ions in ESI and APCI modes (Fig. 5.3). Besides other analyzed compounds, the detection of stearic and pentacosanoic acid methyl esters was optimized and the detection limit in single-ion monitoring mode, based on a *S/N* = 3, was found to be 1.1 pg (APCI) or 1.0 pg (ESI) for stearic, and 0.3 pg (APCI) or 0.2 pg (ESI) for pentacosanoic acid methyl esters, respectively.

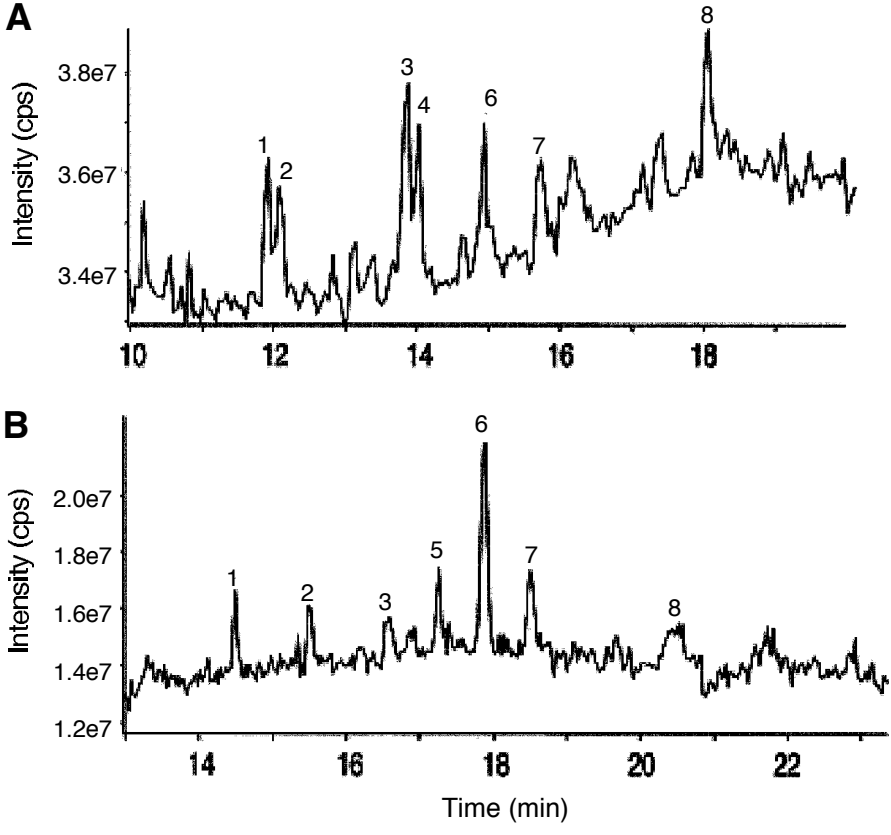

Fig. 5.3. Superctitical-fluid chromatography MS total ion chromatograms of full scans obtained in APCI mode (A) and ESI mode (B). Peaks: 1, stearic acid methyl ester; 3, pentacosanoic acid methyl ester.

Partially hydrogenated fat of commercial origin was analyzed for fatty acids that contained conjugated dienes (5). The peaks eluted from the HPLC and having the conjugated diene chromophore were analyzed by MS. Protonated molecular species, $[M+H]^+$, and ammoniated molecular species, $[M+NH_4]^+$, were detected for all analytes. The molecular mass of each FAME could be determined, but the use of a single quadrupole instrument with a soft ionization source precluded determination of the geometry and position of the double bonds in the fatty chains. For instance, a molecular mass of 294 was obtained for the methyl esters of linoleic acid and for esters of a conjugated linoleic acid (Fig. 5.4). Similarly, a molecular mass of 296 was obtained for the methyl esters of both oleic and elaidic acids (Fig. 5.5).

LC/APCI-MS of Very-Long-Chain Polyunsaturated Fatty Acids (VLCPUFA)

The presence and identity of very-long-chain PUFA from three freshwater crustacean species, *Bathynella natans*, *B. baicalensis*, and *Baicalobathynella magna* from Lake Baikal and caves of Central Europe were determined by means of LC/APCI-MS (6). This method permitted the identification of more than 50 very-long-chain PUFA. These acids, predominantly 26:5ω-6, 28:7ω-6, 30:7ω-3, and 40:7ω-6, were described in the crustaceans for the first time. The mass spectrum of 40:8ω-3, including diagnostic ions, is shown in Figure 5.6.

More recently, the very-long-chain PUFA *allZ*-4,7,10,13,16,19,22,25,28-tetratriacontanonaenoic acid was determined and identified in the freshwater crustacean species *Bathynella natans* living in caves of central Europe by means of LC/APCI-MS (7). The APCI mass spectrum of VLCPUFA had characteristic ions consistent with 34:9 FAME. The pseudomolecular ion $[M+42]^+$ is conventionally taken to be mainly characteristic for PUFA, but in fact it also arises by the addition of acetonitrile from the mobile phase.

However, the determination of position of double bonds was unsuccessful on the basis of the cleavage of nitrogen derivatives (i.e., 4,4-dimethyloxazoline or picolinyl ester; data not shown). Nevertheless, this method was described as successful either for substances with equal chain lengths, but having only one double bond, or for shorter chain compounds having a maximum of eight double bonds and only 28 carbon atoms. In our case, this technique failed, or its results were ambiguous. Therefore, we used the method based on the ratios of ions at *m/z* 109 and 151. The *m/z* 109/151 ratio is near unity and hence the presumed structure is ω-6 (see Fig. 5.7). This was the first time that a FA with nine double bonds was reported as a natural or synthetic product.

The method of enrichment of very-long-chain fatty acids (VLCFA) from total FA of a heterotrophically cultivated green freshwater alga *Chlorella kessleri* and of their identification as picolinyl esters by means of LC/APCI-MS was described by Rezanka (8). This method is based on the use of preparative RP-HPLC of hundred-milligram amounts and their subsequent identification by microbore LC/APCI-MS. A combination of these two techniques was used to identify unusual VLCFA of up

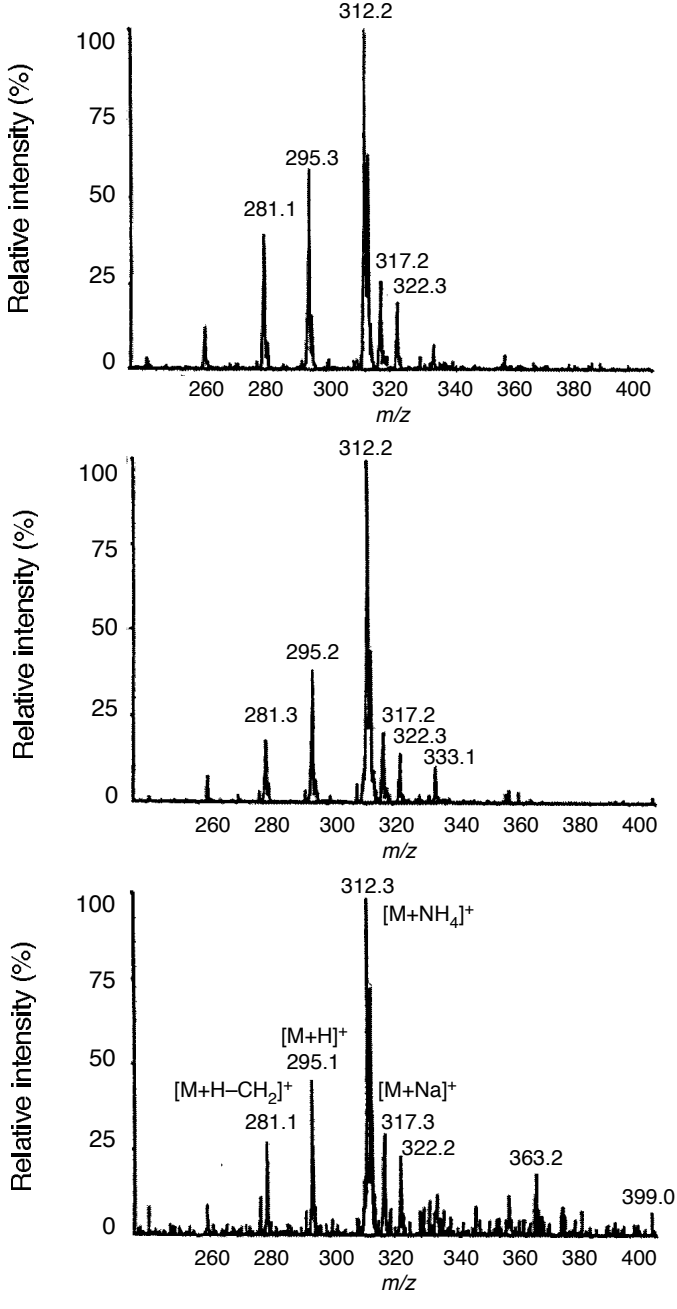

Fig. 5.4. APCI-MS mass spectra of methyl linoleate (upper), and methyl esters of linoleic acid isomers with conjugated dienes (middle and lower).

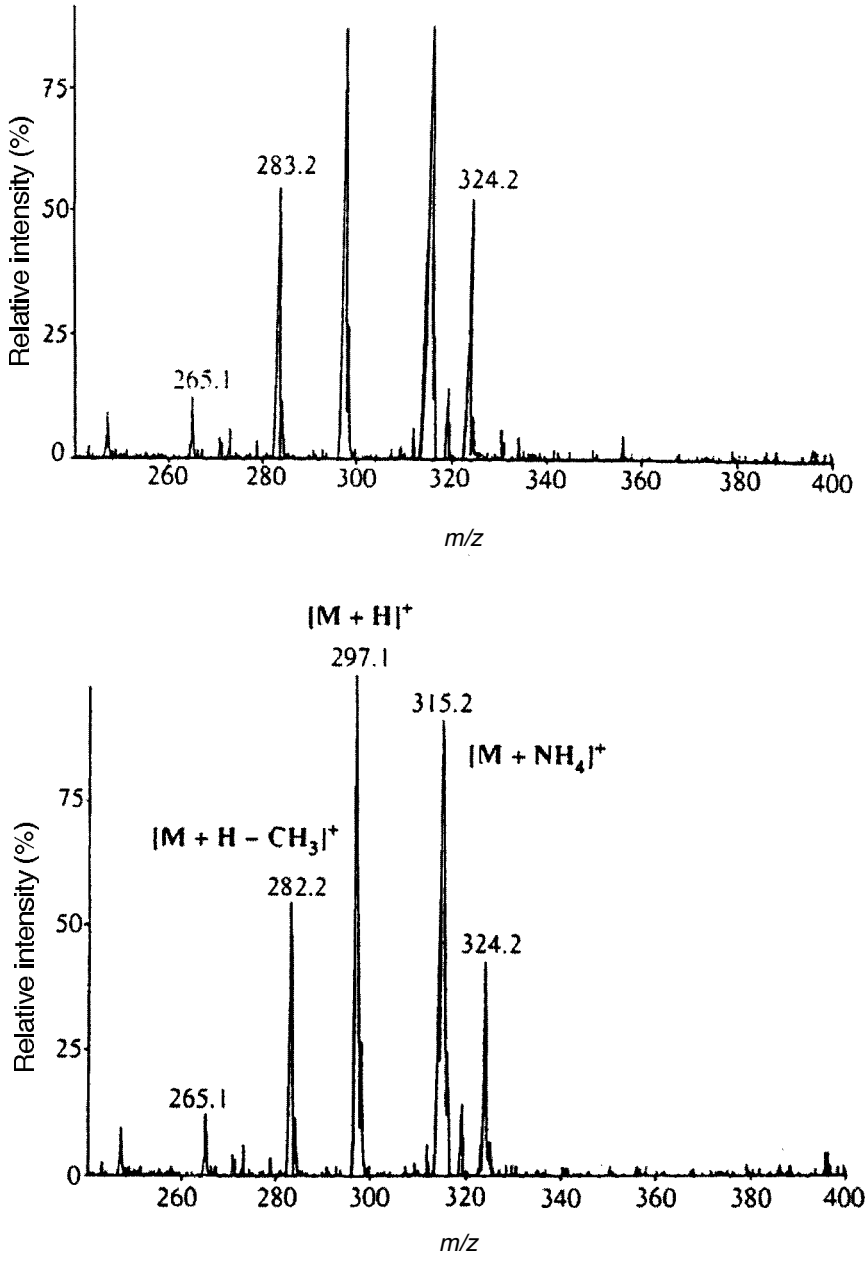

Fig. 5.5. APCI-MS mass spectra of methyl oleate (upper) and methyl elaidate (lower).

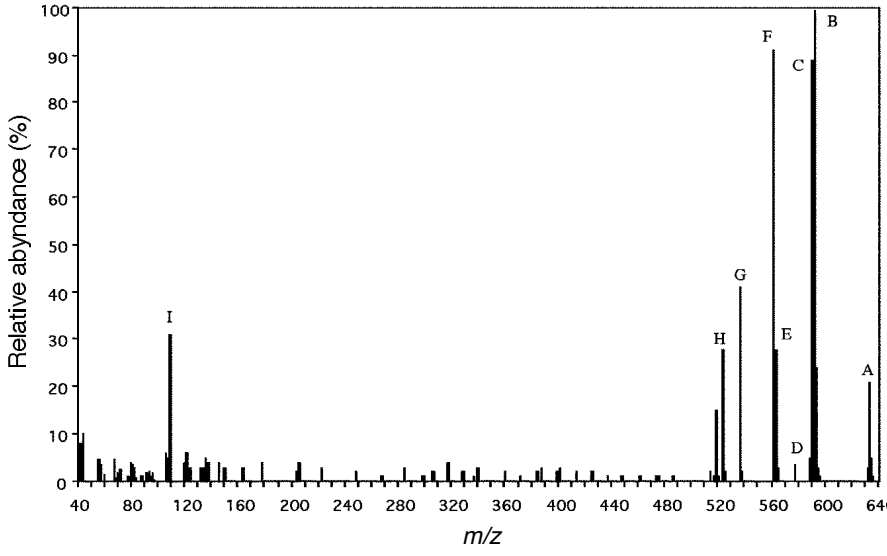

Fig. 5.6. LC-MS (APCI) of 40:8ω3 FAME from *Bathynella natans*. Ions: A $[M+H+ACN]^+$, B $[M+H]^+$, C $[M-H]^+$, D $[M+H-Me]^+$, E $[M+H-Et]^+$, F $[M+H-MeO]^+$, G $[M+H-Bu]^+$, H $[M+H-pentyl]^+$, I *m/z* 109 (diagnostic ion).

to 47 carbons, both saturated and monounsaturated, having two positional isomers (ω-9 and ω-26).

In contrast to EI ionization, in which the mass spectra of the picolinyl esters of straight-chain saturated FA show the most abundant ions in the lower part of mass spectra, that is, ions at *m/z* 92, 108, 151, and 164, these ions are in the minority in APCI, as shown in Figure 5.8 (e.g., 43:0). Even-numbered ions differing by 14 amu and representing the products of cleavage between methylene groups also have low intensities. A different situation can be found in the M^+ region. Here we can observe the formation of two abundant ions: $[M-H]^+$ and $[M+H]^+$, as well as the generation of adducts with the mobile phase such as $[M+40]^+$ or $[M+C_2H_2N]^+$ and $[M+54]^+$ or $[M+C_3H_4N]^+$. In all investigated VLCFA spectra, the ion $[M+H]^+$ is the most abundant.

In the case of monoenoic derivatives, the ions $[M-H]^+$, $[M+H]^+$, $[M+40]^+$, and $[M+54]^+$ were also very abundant in the M^+ region. A large difference in ion distribution was found with the $[M-H]^+$ ion, which exhibited a threefold higher intensity in monoenoic VLCFA than in saturated VLCFA. The 38:1 FA, the mass spectrum which is shown in Figure 5.9, represents a mixture of two positional isomers in a ratio of approximately 1:1. Detection of ions at *m/z* 262, 276, and 302 and at 500, 514, and 540 pointed to the presence of a mixture of two positional isomers, ω-9 and ω-26.

The study reported by Holcapek and colleagues (9) concerned the identification by LC/APCI-MS of the individual compounds after partial reesterification of plant oil used as a biofuel. The pseudomolecular ions, $[M+H]^+$, were observed for

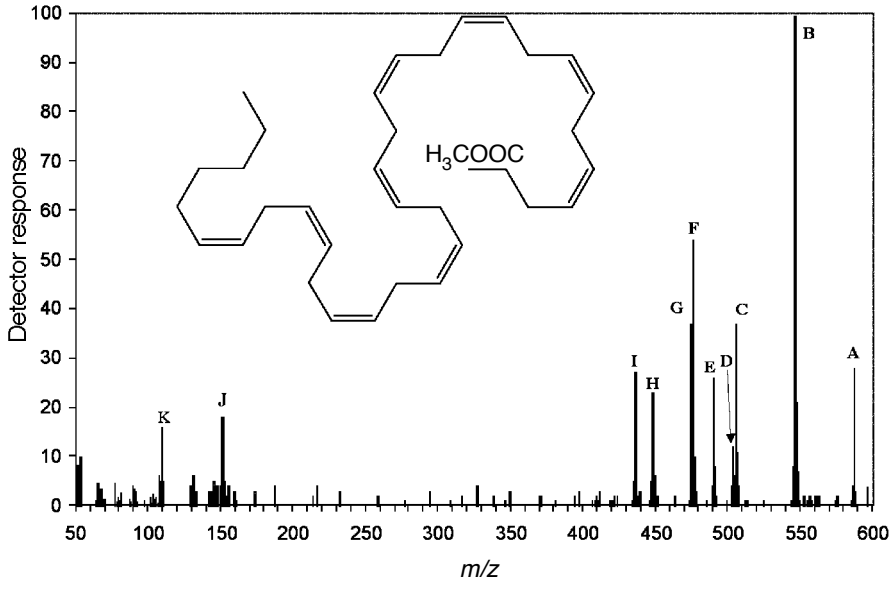

Fig. 5.7. LC/APCI-MS of 34:9ω6 FAME from *Bathynella natans*. Ions (abundance): (A) $[M+H+2\times CH_3CN]^+$, *m/z* 587 (28); (B) $[M+H+CH_3CN]^+$, *m/z* 546 (100); (C) $[M+H]^+$, *m/z* 505 (37); (D) $[M-H]^+$, *m/z* 503 (12); (E) $[M+H-CH_3]^+$, *m/z* 490 (26); (F) $[M+H-C_2H_5]^+$, *m/z* 476 (54); (G) $[M+H-CH_3O]^+$, *m/z* 474 (37); (H) $[M+H-C_4H_9]^+$, *m/z* 448 (23); (I) $[M+H-C_5H_9]^+$, *m/z* 436 (27); (J) *m/z* 151 (18) (diagnostic ion); (K) *m/z* 109 (16) (diagnostic ion).

all eluted compounds. In addition to these ions, a series of aliphatic ions similar to those obtained by conventional EI-MS were observed in the spectra of FAME under the ionization conditions used.

LC/APCI-MS of Fatty Acids and Resin Acids

LC-MS-based methods were developed for the analysis of 10 resin acids and five FA in process waters from paper industries (10). No fragmentation of target compounds was observed using APCI with negative ionization. The $[M-H]^-$ ions permitted the individual quantification of fatty and aromatic resin acids. Limits of detection were ~0.1 ng for all compounds. Changes in parameters that were common for the two interfaces, such as the drying gas temperature, nebulizer pressure, capillary voltage, and cone voltage, caused only insignificant differences in the mass spectra. In contrast, an increase in the corona current from 4 to 10 μA increased the response and a value of 8 μA was selected, which led to slightly higher sensitivities for most compounds. Once the MS parameters had been optimized for each interface, the responses obtained for the target compounds under the optimal conditions were compared.

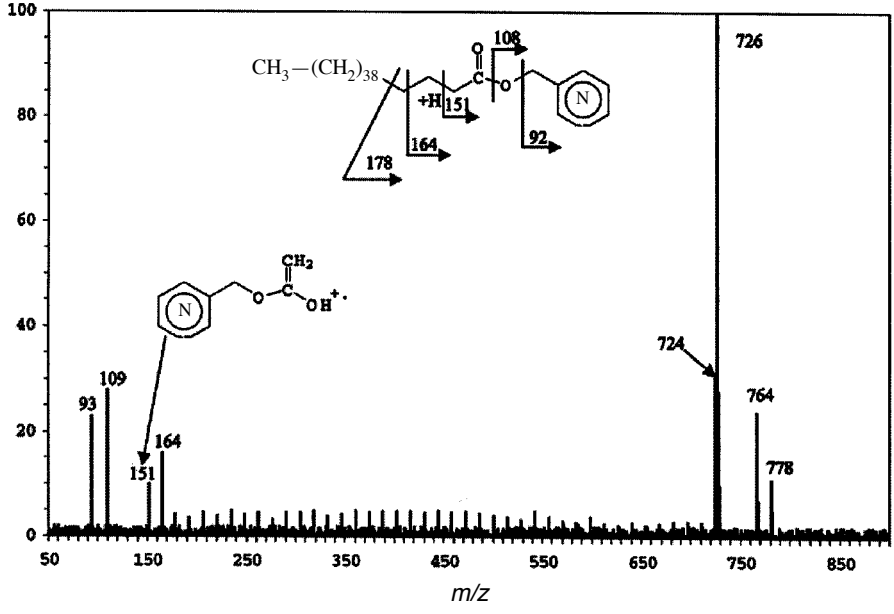

Fig. 5.8. APCI-MS mass spectrum of the picolinyl ester of 43:0 acid; the structures of major ions are shown.

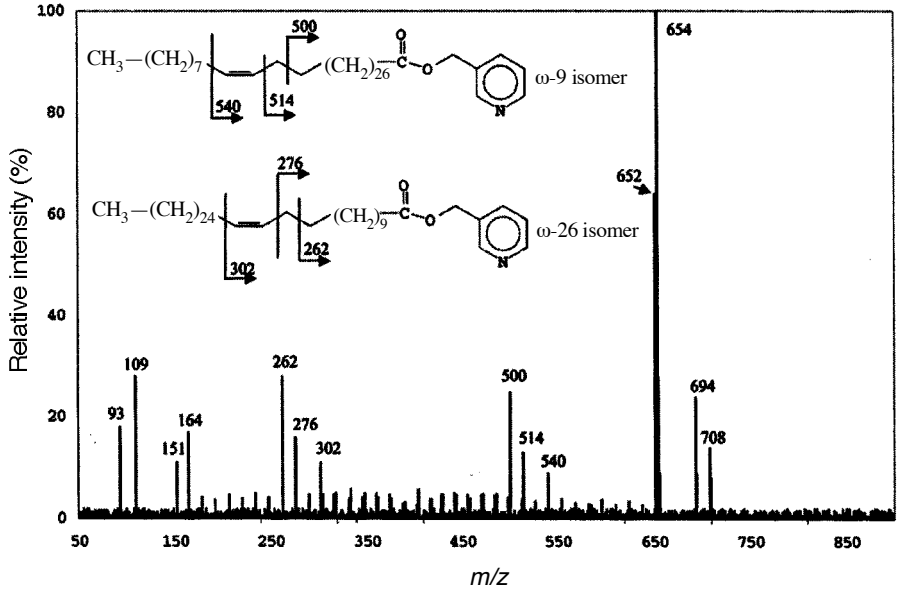

Fig. 5.9. APCI-MS mass spectrum of the picolinyl ester of a 38:1 fatty acid mixture; the structures of major ions are shown.

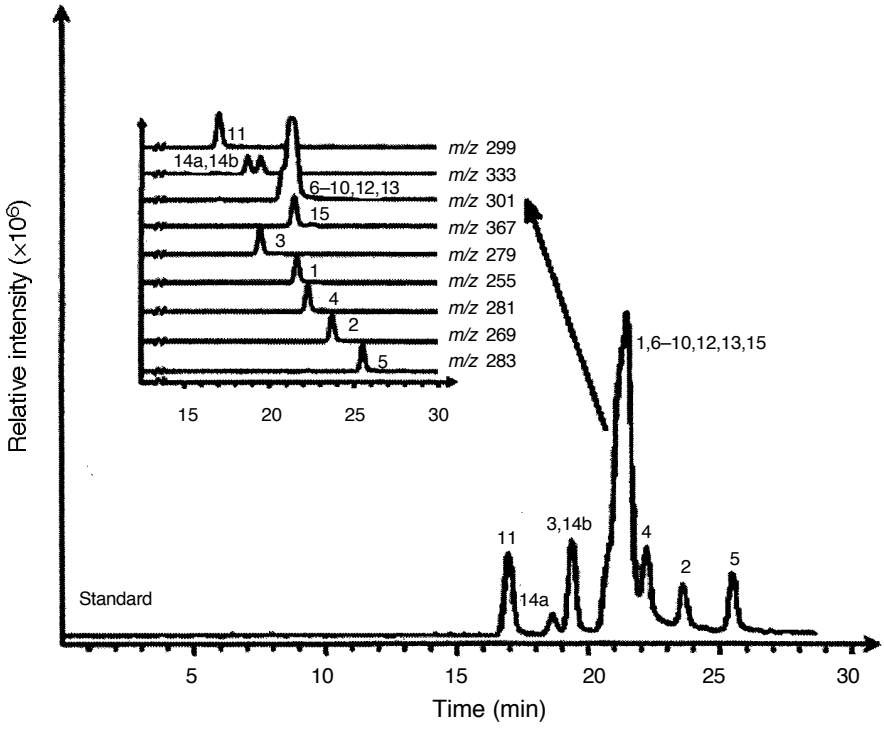

Fig. 5.10. Total-ion chromatogram from LC/APCI-MS in SIM mode of the five fatty acids and the 10 resin acids (16 ng injected). Acids: 1 = palmitic; 2 = margaric; 3 = linoleic; 4 = oleic; 5 = stearic; 6–15 resins' acids.

A comparative study (11) of the performance of LC/APCI-MS and GC-MS for the determination of resin and fatty acids from paper mill process waters (Fig. 5.10) also reported the limits of detection, recoveries, reproducibility, linearity, and precision of both methods. Although LC/APCI-MS involved coelution of the nonaromatic resin acids, it also showed good sensitivity (limits of detection ~3 μg/L) and permitted the detection of resin and fatty acids at the μg/L level.

LC/APCI-MS for Oxidized FA

The FA and FAME commonly encountered in commercial vegetable oils were tested as substrates for immobilized peroxygenase enzyme from oat (*Avena sativa*) seeds, and the epoxide products were characterized by LC/APCI-MS (12). All reaction products were examined by using MS coupled with LC or GC, and the authors were able to demonstrate that the oat seed peroxygenase exhibited specificity for epoxide formation with no other products being detected (Table 5.1). It was evident that all spectral data included the following ions: $[M+H+ACN]^+$, $[M+H]^+$, $[M+H–H_2O]^+$, $[M+H–MeOH]^+$, and $[M+H^+–H_2O–MeOH]^+$.

TABLE 5.1
Tabulated Mass Spectra of Epoxides

Substrate	RT (min)	APCI-MS	Product
2 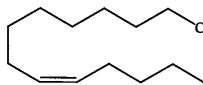	30.50	*m/z* 354 [M+42 (+H^++ACN)], 313 [M+1], 295 [M+1–18 (+H^+–H_2O)], 263 [M–49, (+H^+–H_2O–MeOH]	2a
3 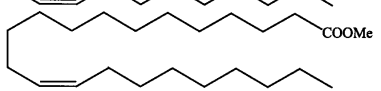	43.50	*m/z* 410 [M+42], 369 [M+1], 351 [M–17], 337 [M–31, (+H^+–MeOH)], 319 [M–49]	3a
4 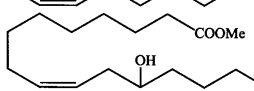	12.16	*m/z* 370 [M+42], 329 [M+1], 311 [M–17], 293 [M–35, (+H^+–2H_2O)], 279 [M–49]	4a
5	27.18	*m/z* 352 [M+42], 311 [M+1], 293 [M–17], 279 [M–31], 262 [M-49]	5a (9,10-epoxy)
6 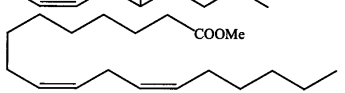	27.42	*m/z* 352 [M+42], 311 [M+1], 293 [M–17], 279 [M–31], 261 [M-49]	5b (12,13-epoxy)
	18.07	*m/z* 368 [M+42], 327 [M+1], 309 [M–17], 296 [M–31], 222 [M-49]	5c (diepoxy)
7 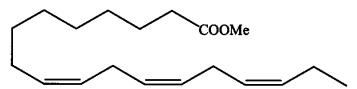	23.28	*m/z* 350 [M+42], 309 [M+1], 291 [M–17], 277 [M–31], 259 [M–49]	7a (monoepoxy)
	12.54	*m/z* 366 [M+42], 325 [M+1], 307 [M–17], 293 [M–31], 275 [M–49]	7b (9,10–15,16-diepoxy)

LC/APCI-MS was developed (13) as an alternative method for characterization of hydroxylated metabolites of oleic and elaidic acids in rat and human liver microsomes.

Oxidation of oleic and elaidic acids led to the formation of two main metabolites, which were identified as ω- and (ω-1)-hydroxylated (or 17-OH and 18-OH) fatty acids on the basis of their pseudomolecular ions and their fragmentation. The assay was accurate and reproducible, with a detection limit of 25 ng per injection. LC/APCI-MS offers considerable advantages since the method does not require the use of a radioactive molecule, completely separates the two hydroxymetabolites, confirms the identification of each metabolite, and is as sensitive as radiometric analysis.

The corresponding mass spectra of OH-FA and the elaidic acid are shown in Figure 5.11. The OH-FA were characterized by a deprotonated molecule ion, $[M–H]^-$, at *m/z* 297; elaidic acid also exhibited a deprotonated molecule ion at *m/z* 281.

LC/APCI-MS of FA Amide Derivatives

A useful method for analyzing FA by LC/APCI-MS has been developed (14). The sensitivity of determination of six kinds of palmitamide derivatives monitored by

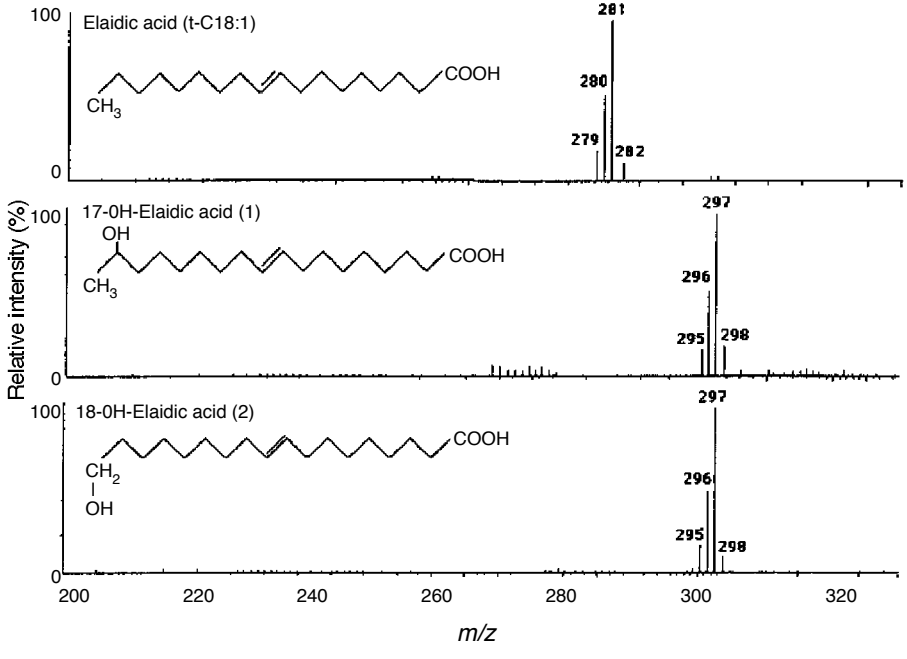

Fig. 5.11. APCI-MS mass spectra (negative ion mode) of elaidic acid and its hydroxylated metabolites.

the single $[M+H]^+$ ion was, in decreasing order: *N-n*-propylamide > anilide > *N,N*-diethylamide ~ *N,N*-diphenylamide > *N*-l-naphthylamide. This method was used to detect both hydroxy and nonhydroxy FA (e.g., from 16:0 to 30:0). Many kinds of FA, including hydroxy FA of the rat brain, were detected in a single run.

N,N-propylamide derivatives exhibited a single and intense $[M+H]^+$ ion. In the mass spectra of *N,N*-diethylamide, $[M+H]^+$ ions were also observed as the base peaks. The mass spectra of *N*-l-naphthylamide or *N,N*-diphenylamide derivatives contained, in addition to $[M+H]^+$ ions, ions at *m/z* 144 $[C_{10}H_7NH_2+H]^+$ and *m/z* 170 $[(C_6H_5)_2NH+H]^+$, respectively, arising from cleavage of the amide group. The mass spectra of 2-hydroxy FAs showed intense $[M+H]^+$ ions as base peaks, whereas those of 12-hydroxy FA showed $[M+H]^+$ ions but had $[M+H-H_2O]^+$ ions as base peaks (Fig. 5.12).

A simple and selective LC/APCI-MS method was developed (15) for the determination of anandamide (arachidonoylethanolamide), an endogenous cannabinoid

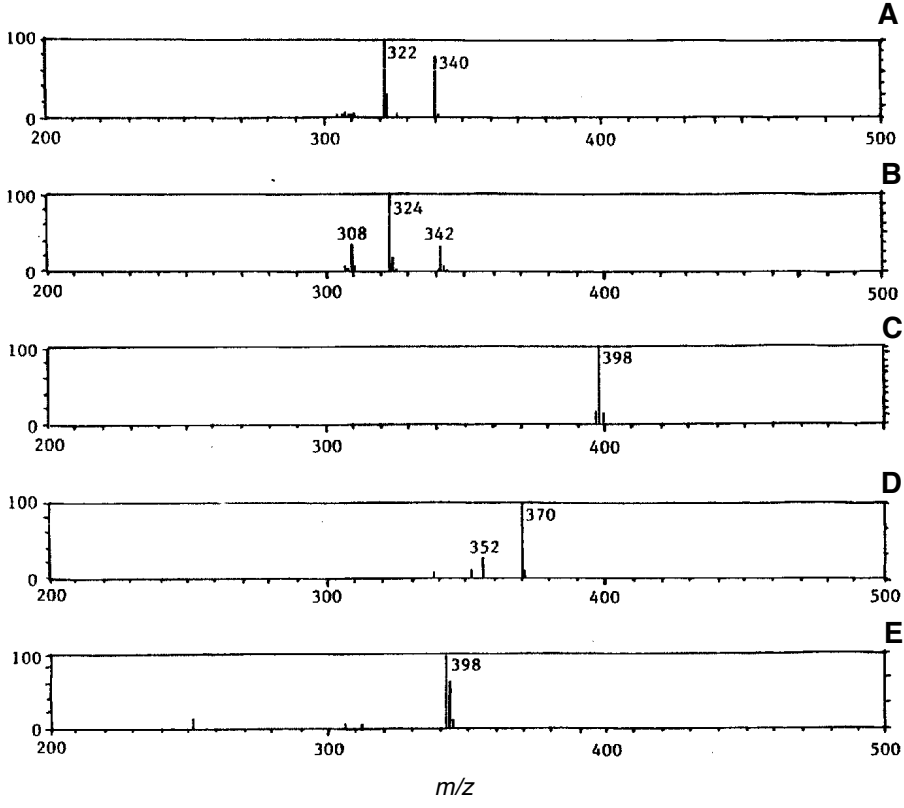

Fig. 5.12. APCI-MS mass spectra of different *N-n*-propylamide derivatives: (A) 12-OH-18:1, (B) 12-OH-18:0, (C) 2-OH-22:0, (D) 2-OH-20:0, (E) 2-OH-18:0.

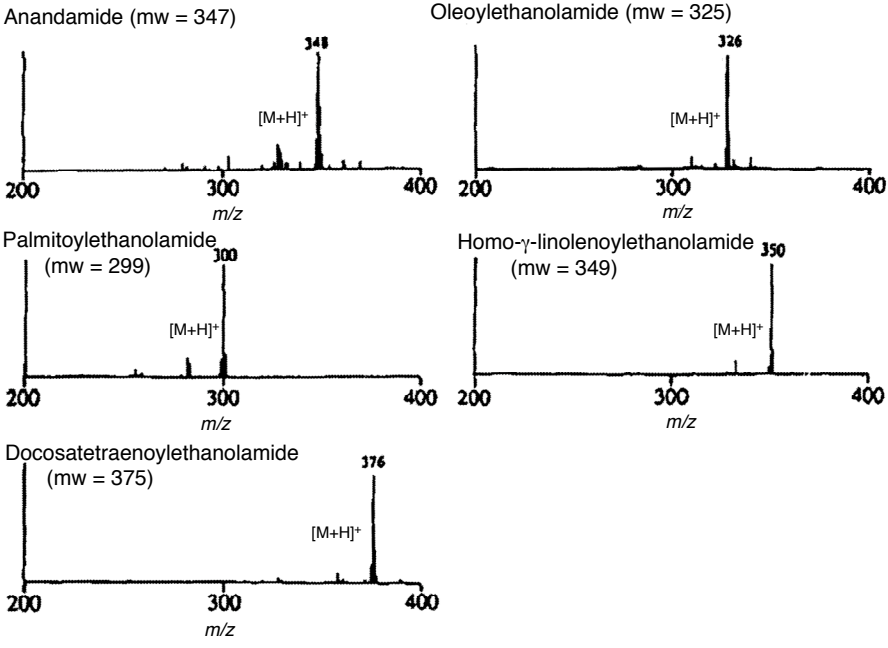

Fig. 5.13. APCI-MS mass spectra of anandamide and its analogs.

receptor ligand, and its analogs. The calibration curve for standard anandamide was linear over the range of 625 fmol to 125 pmol and the detection limit was 200 fmol per injection at a signal-to-noise ratio of 2. The mass spectra obtained from anandamide and its analogs are shown in Figure 5.13. All of them produced protonated molecule ions as the base-peak ions at *m/z* 348 (anandamide), *m/z* 300 (palmitoylethanolamide), *m/z* 326 (oleoylethanolamide), *m/z* 350 (homo-γ-linolenoylethanolamide), and *m/z* 376 (docosatetraenoylethanolamide). To optimize APCI conditions, the effects of the drift voltage and the nebulizer temperature on anandamide ion production were examined. The intensity of $[M+H]^+$ decreased as the drift voltage increased, while the intensity of $[M+H-H_2O]^+$ increased. The maximum intensity of $[M+H]^+$ was observed when the drift voltage was set at 20 V. The temperature for which the $[M+H]^+$ intensity was at a maximum was around 200°C. Similar results were obtained for anandamide analogs.

Other Applications of LC/APCI-MS to PUFA

LC/APCI-MS analysis proved to be a method superior to GC-MS in the identification of PUFA chain length and degree of unsaturation (16). Based on the unequivocal presence of the protonated molecule ion and characteristic acyl daughter ions, 20:5 was clearly identified from *Shewanella pealeana* (Fig. 5.14). LC/APCI-MS analysis also resulted in the detection of previously unidentified unsaturated com-

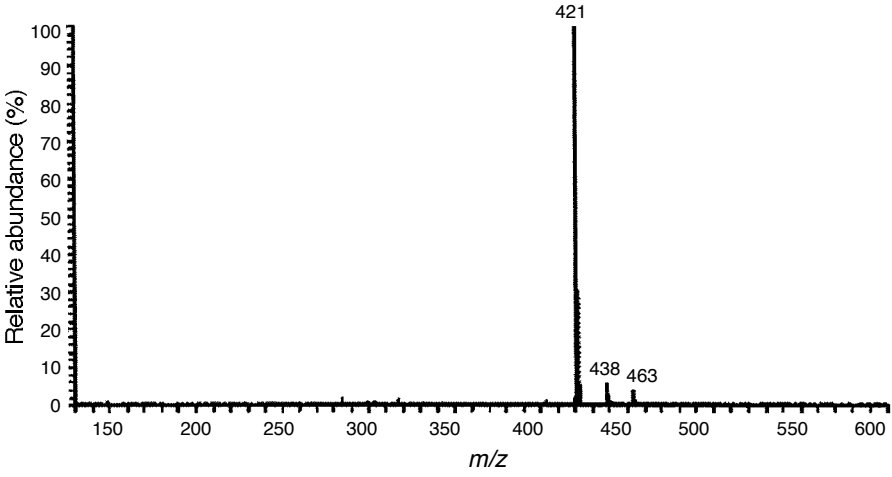

Fig. 5.14. APCI-MS mass spectrum of 20:5 2-oxo-phenylethyl ester from *S. pealeana*.

ponents. A 16:4 PUFA was detected and identified from the characteristic protonated molecule at *m/z* 367. Further PUFA components (18:4 and 22:5) were also clearly identified by LC-MS analysis from the presence of the characteristic protonated parent and MS-MS daughter ions.

The LC retention times also provided confirmatory support for the assignment of these and other rare or novel PUFA. The correlation of retention time with unsaturation for the C_{22} chain series from menhaden oil demonstrated the powerful ability of the LC/APCI-MS system to directly identify PUFA by the protonated molecules (Fig. 5.15). The correlations based on both chain length and degree of unsaturation were also demonstrated for another series of PUFA from menhaden oil including 28:8, 28:7, 28:6, 26:7, 26:6, 26:5, 26:4, 24:6, and 24:5. Any potential ambiguity for FA of the same molecular mass (e.g., 27:1 and 28:8) was eliminated by observation of retention times.

Ionization and detection of PUFA by LC/APCI-MS provided a significant benefit in detection ability when compared to ultraviolet (UV) detection (approximately 20 to 30 times stronger response relative to 16:0). Analysis of a menhaden oil standard containing the unsaturation series 16:0 to 16:4 demonstrated that the degree of enhanced detection was approximately proportional to the number of double bonds, in addition to a small effect of chain length (Table 5.2). Tests with a pure DHA phenacyl ester standard gave an absolute detection limit in full-scan mode of 200 pg, comparable with UV detection of the pure standard. In the selected reaction-monitoring mode, the detection limit for docosahexaenoic phenacyl ester based on the acyl daughter ion at *m/z* 311, derived from the molecular ion, was 5 pg. This limit is essentially independent of whether the sample is a standard or a complex mixture of FA.

LC/APCI-MS was used to analyze FA split off from lecithins after phospholipase A treatment and also some hydroperoxy FA split off from photo-oxidized

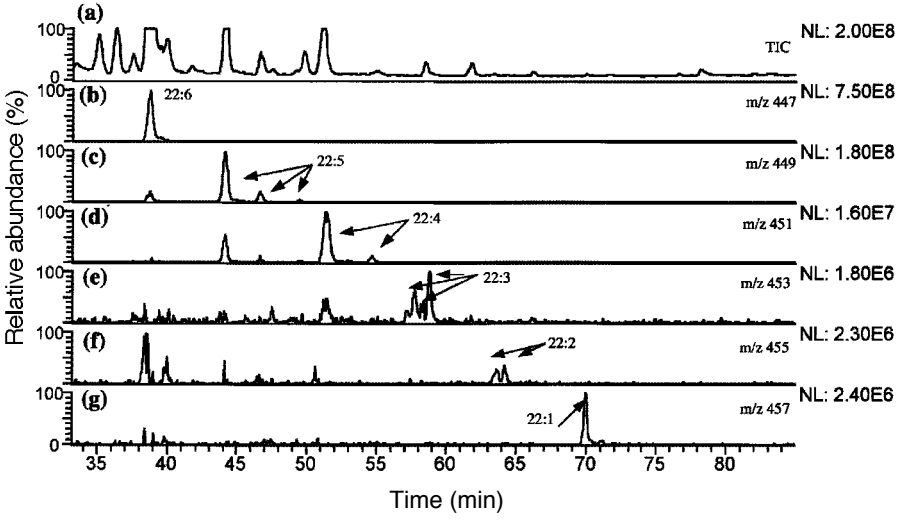

Fig. 5.15. Total ion chromatogram (a) and mass chromatograms (b–f) of the $[M+H]^+$ ions for the C_{22} 2-oxo-phenylethyl esters of menhaden oil.

lecithin. The pseudomolecular ions $[M+H]^+$ in 7-methoxy-1,4-benzoxazin-2-one-3-methyl derivatives (MB; see Fig. 5.16) were the base peaks. Ions observed at *m/z* 231 in mass spectra of these MB derivatives are assumed to be ions of (MB+ACN) (17). No significant difference was observed between the spectra of saturated and unsaturated FA.

TABLE 5.2
Relative Response Factors (Relative to the Detection of 16:0) for APCI-MS Detection Versus UV Detection of Fatty Acid 2-oxo-Phenylethyl Esters from a Menhaden Oil Standard and *S. pealeana*

Fatty acid	Response factor
16:4	19.5
16:3	23.6
16:2	2.7
16:1	3.6
16:0	1.0
18:4	23.2
20:5	23.2
22:5	31.6
22:6	25.7
18:0	1.04
16:0	1.00
14:0	0.88

An $[M+H-H_2O]^+$ ion (base peak) accompanying a smaller pseudomolecular ion $[M+H]^+$ was observed in the mass spectrum of the 12-OH-18:0 MB (Fig. 5.17). The spectrum of the 2-OH-18:0 MB derivative was similar. The sensitivity of the palmitic acid MB derivative was determined by monitoring the single $[M+H]^+$ ion and amounts as low as 5 ng of palmitic acid could be detected.

FA esters of 3-(*N*-phenylamino)-1,2-propanediol were considered the best chemical markers of toxic oils related to the Spanish toxic oil syndrome (18). Their analysis was based on solid-phase extraction using strong anion-exchange cartridges, followed by LC/APCI -MS-MS quantification. Quantitative measurements were performed by two different internal standards (Table 5.3): compound 4 for quantification of the monoesters and compound 9 for the diesters of compound 1. Analyses were performed in the precursor-ion scan mode. $[M+H]^+$ ions at *m/z* 432, 420, 684.5, 692.5, 694.5, and 696.5 (for compounds 3, 4, 9, 5, 6, and 8, respectively) were selected in the first quadrupole and the common product ion at *m/z* 132 was monitored in the second analyzer (Fig. 5.18).

In a sphingomyelin-enriched sample of polar lipids from bovine milk, molecular species of intact sphingomyelin were separated by LC-MS (19). In-source fragmentation of sphingomyelin ions by positive APCI led to the formation of ceramide ions. With the ceramide ions as precursors, ions representative of both the long-chain base parts and the FA parts were detected in APCI-MS-MS. By using this procedure, it was possible to determine the sphingomyelin molecular mass and then the respective long-chain base (LCB)-FA combination(s) by using APCI(+)-MS-MS. At least 36 protonated molecules of intact sphingomyelin were detected in the bovine milk sample. The combinations found covered a range of molecular masses from 673 to 815. The 12 most common protonated molecules were composed of at least 25 different LCB-FA combinations. Saturated and unsaturated LCB and FA were detected in addition to hydroxy FA. The most common LCB were 16:1, 17:1, 18:1, and 19:1, whereas the most common FA were 16:0, 22:0, 23:0, and 24:0.

LCB-FA combinations of sphingomyelin from bovine brain, bovine erythrocytes, and chicken egg yolk were also identified. For positive-ion APCI, the mass spectra were more complex than for ESI because of extensive in-source fragmentation (Fig. 5.19). For sphingomyelin 18:1/18:0, the base peak appeared at *m/z* 548, corresponding to protonated molecules with a loss of phosphorylcholine, $[M+H-183]^+$ (the M-183 part is hereafter denoted Cer, ceramide).

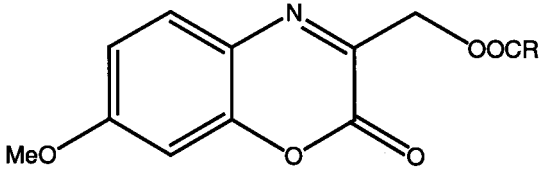

Fig. 5.16. Structure of 7-methoxy-1,4-benzoxazin-2-one-3-methyl (MB) ester of fatty acid.

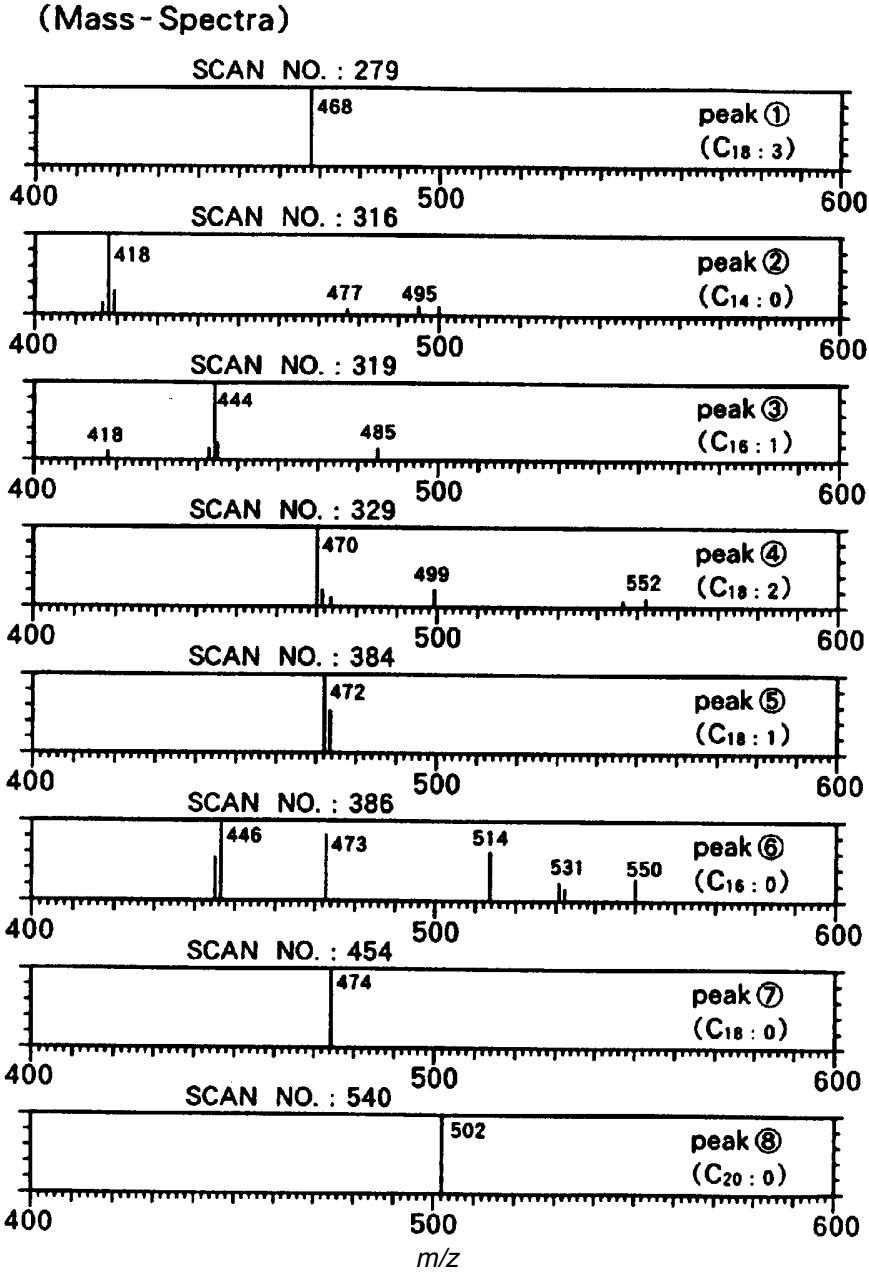

Fig. 5.17. LC-MS mass spectra of the MB derivatives of fatty acids. A mixture of eight kinds of fatty acids (approximately 10 nmol each 14:0, 16:0, 16:1, 18:0, 18:1, 18:2, 18:3, and 20:0) was used.

TABLE 5.3
Structures and Names of Different of Toxic Compounds

Compound	Chemical name	$(M+H)^+$
1	3-(*N*-phenylamino)-1,2-propanediol	168
2	2-hydroxy-3-(*N*-phenylamino)propyl linoleate	430
3	2-hydroxy-3-(*N*-phenylamino)propyl oleate	432
4	2-hydroxy-3-(*N*-phenylamino)propyl heptadecanoate	420
5	2-linoleoyl-3-(*N*-phenylamino)propyl linoleate	692
6	2-oleoyloxy-3-(*N*-phenylamino)propyl linoleate	694
7	2-linoleoyl-3-(*N*-phenylamino)propyl oleate	694
8	2-oleoyloxy-3-(*N*-phenylamino)propyl oleate	696
9	2-oleoyloxy-3-(*N*-phenylamino)propyl heptadecanoate	698

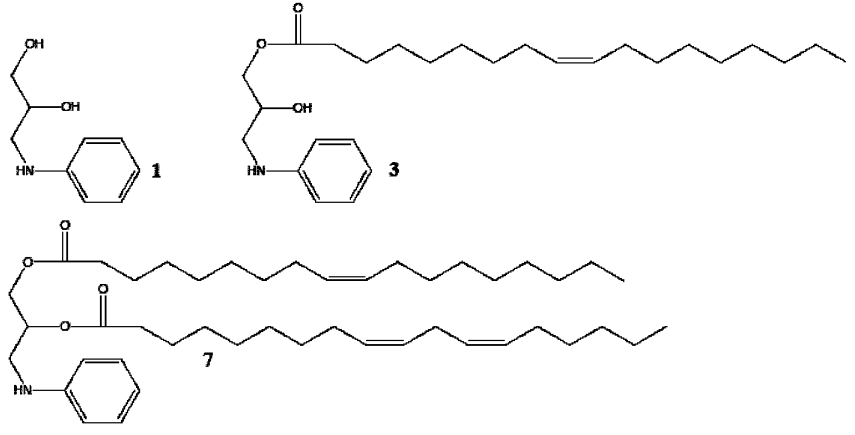

In addition to $[Cer+H]^+$, also $[Cer+H–H_2O]^+$, $[Cer+Na]^+$, and $[Cer+K]^+$ were abundant. In the molecular ion region, $[M+H–CH_2]^+$ ions of *m/z* 717 were obtained (formed presumably in a substitution reaction in which one methyl group is replaced by hydrogen). Also, $[M+H–CH_2–H_2O]^+$ and $[M–CH_2+Na]^+$ were obtained. Prominent ions of *m/z* 654 were tentatively assigned as $[M+H–N(CH_3)_3–H_2O]^+$ wherein one molecule of water was lost from the LCB. In the low-mass region, ions of *m/z* 184 corresponding to phosphorylcholine were observed, as in the positive ESI mode. Similar results were obtained for the other sphingomyelin standards. In APCI with negative-ion detection, the mass spectra (not shown) were reported to be comparable to those obtained in negative-ion ESI but with lower sensitivity.

Lipid extracts of archaeological shards from late Roman cooking pots were analyzed by using LC/APCI-MS (20). This advanced technique showed the use of beeswax through identification of the constituting alkanes and mono- and diesters. Part of the animal fat was characterized as originating from ruminants because of the presence of *trans* FA. The results illustrate how the compositions of complex mixtures can be unraveled and the original contents of ancient ceramic vessels can be determined by using specialized analytical equipment.

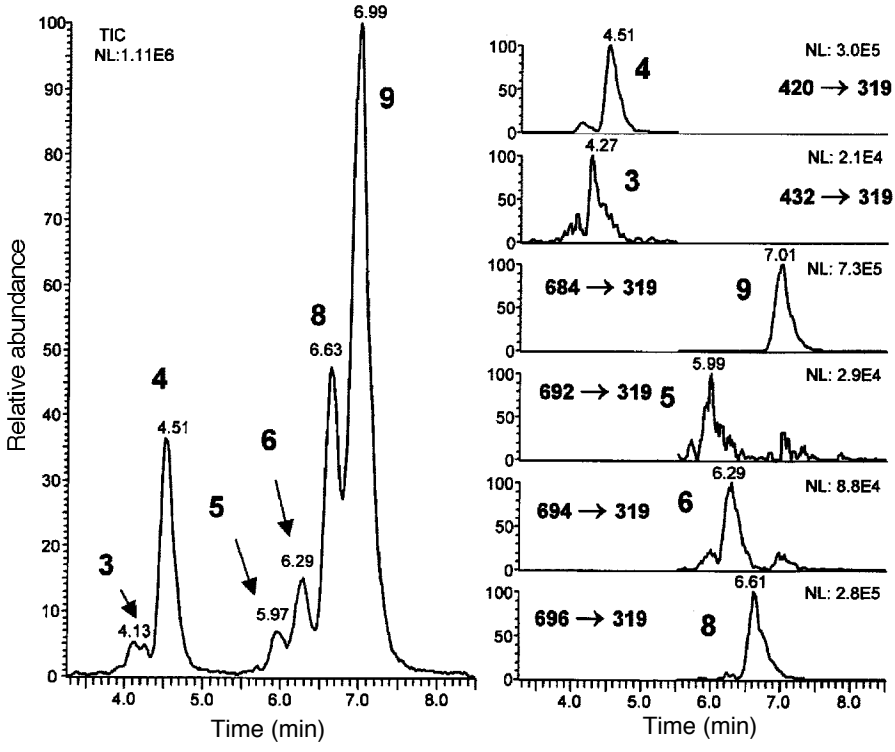

Fig. 5.18. LC-APCI-MS/MS chromatogram (left) and extracted ion chromatograms (right) corresponding to the analysis of toxic oil syndrome-related oil sample.

The saturated monoesters were the most important compounds of beeswax and consisted of long-chain alcohols (C_{24}–C_{36}) esterified with palmitic acid. The hydroxymonoesters coeluted with monoesters of a similar carbon number and the monoesters with a larger carbon number (C_{46}–C_{50}) coeluted with hydroxydiesters.

The most important fragment ions of the saturated monoesters (alkyl palmitates) were characterized by an intense hydride-extracted molecular ion $[M–H]^+$ and $[C_{15}H_{31}COOH–H]^+$ ion formed by the loss of the FA. Also, the acylium ion of palmitic acid at *m/z* 237, $[C_{15}H_{31}COO–H_2O]^+$, was detected. No distinction could be made between the mass spectrum of saturated and unsaturated monoesters, since unsaturated monoesters form abundant $[M+H]^+$ ions. Hydroxymonoesters eluted just after the saturated monoesters and showed hydride-extracted molecular ions, $[M–H]^+$, and the hydroxy-palmitic acid ion $[C_{15}H_{30}OHCOOH–H]^+$, formed by the loss of the FA. The diesters (C_{56}–C_{64}) showed an abundant $[M+H]^+$ ion and intense fragment ions caused by the loss of palmitic acid, $[M+H–C_{15}H_{31}COOH]^+$. Also, hydroxydiesters were detected, which showed an $[M+H]^+$ ion together with an $[M+H–C_{15}H_{30}\ OHCOOH]^+$ ion formed by the loss of hydroxy-palmitic acid.

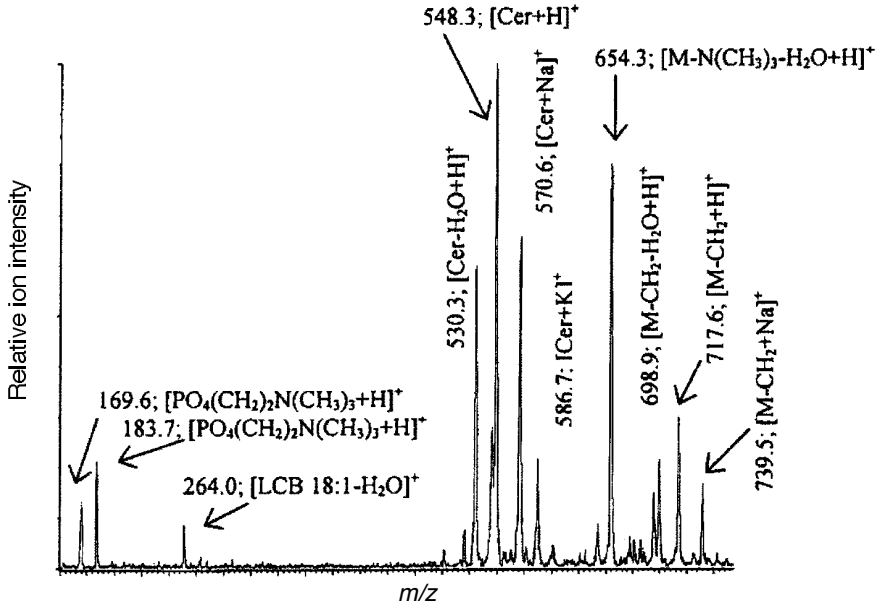

Fig. 5.19. APCI mass spectrum of *d*-18:1/18:0-sphingomyelin.

Vitamin Metabolites by LC/APCI-MS

The separation of possible metabolites of vitamin D_3, that is, 3-stearate, 3-palmitate, 3-oleate, and 3-linoleate, was performed by using LC/APCI-MS (21). The FA esters were derivatized with a Cookson-type reagent (4-phenyl-1,2,4-triazoline-

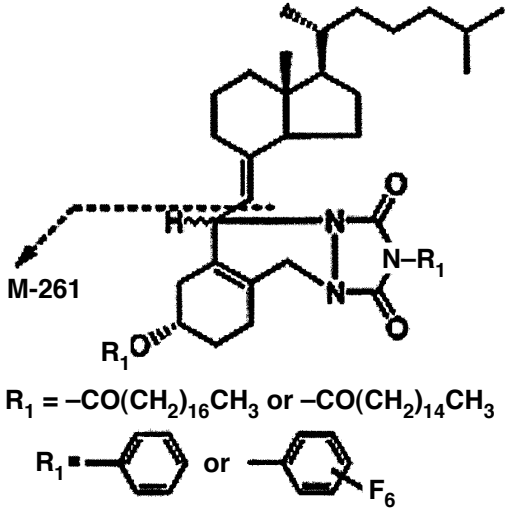

Fig. 5.20. Fragmentation of adducts of D_3 3-fatty acid esters with Cookson-type reagents.

3,5-dione) to give stable Diels-Alder adducts (PTAD) (Fig. 5.20) and they showed a quasimolecular ion as an intense peak.

Endogenous vitamin D_3 is present mainly in urine and serum in a nonpolar esterified form. The LC/APCI-MS of these esters showed their deesterified ion (*m/z* 367) as a base peak in the positive-ion mode, but pseudomolecular ions (*m/z* 651 and 623, respectively) were also detected with weak intensity (<12%). In the negative mode, these esters did not show any characteristic ions (Table 5.4).

The adducts with PTAD showed pseudomolecular ions with relatively strong intensities (>53%), together with the corresponding $[M–261]^+$ ions as base peaks in positive-ion mode. It may be postulated that these fragment ions were formed by cleavage at the $C_{6–7}$ bond of the D skeleton and loss of the CD-ring with a side chain, which can be used to identify the FA moiety of these esters. In the negative-ion mode, PTAD adducts showed pseudomolecular ions or cluster ions, which were postulated as the addition of a Cl^- ion derived from $CHCl_3$ used as an injection solvent.

Separation and characterization of 3-FA esters of pregnenolone and dehydroepiandrosterone in rat brain were performed by using LC/APCI-MS operating in the positive-ion mode (22). The FA esters obtained from the rat brain were derivatized with *O*-methyl-hydroxylamine to give the respective methyloximes, which were identified by comparing their chromatographic retention times with those of authentic samples during LC/APCI-MS.

The xanthoside composition of the crude extract of *Umbilicaria proboscidea* was characterized by using LC-UV diode array detection and LC/APCI-MS methods (23). The presence of acylated xanthone-*O*-glucosides was determined by both positive- and negative-ion LC/APCI-MS. Based on UV and MS spectral data and nuclear magnetic

TABLE 5.4
LC-APCI-MS Data on D_3 3-Fatty Acid Esters and Their Adducts with Cookson-type Reagents

		Observed ion (*m/z*)	
Compound	M.W.	Positive	Negative
D_3 3-Stearate	650	367.4 $[M+H–C_{18}H_{36}O_2]^+$ (100)[a] 651.7 $[M+H]^+$ (10)	ND[b]
PTAD[c]	825	564.5 $[M–261]^+$ (100) 826.7$[M+H]^+$ (93)	319.1(100) 860.5 $[M+35]^-$ (76)
D_3 3-Palmitate	622	367.4 $[M+H–C_{16}H_{32}O_2]^+$ (100) 623.6 $[M+H]^+$ (12)	ND
PTAD	797	536.4 $[N–261]^+$ (100) 798.8 $[M+H]^+$ (53) 886.6 $[M–1]^+$ (61)[d]	796.9 $[M–H]^-$ (20) 832.6 $[M+35]^-$ (100)

[a]Relative intensity (%).
[b]Not detected.
[c]Adduct.
[d]Ambiguity still remains in this ion's identification.

resonance (NMR) spectroscopy, a total of 14 compounds (6-*O*-acylated umbilicaxanthosides A and B) were identified in *U. proboscidea* for the first time. To further develop the applicability of LC-MS techniques to phytochemical characterization, the effect of different ionization energies on fragmentation was studied using APCI-MS. Optimal ionization conditions were achieved with positive-ion APCI using ammonium acetate buffer, and with negative-ion APCI by using formic acid (pH 4).

The (2,4-dinitrophenyl)hydrazones of 1-alkanals (from formaldehyde to octadecanal) and other carbonyl compounds were separated by LC/APCI-MS (24). The base peak in the negative-ion APCI mass spectrum was the $[M–H]^-$ ion $(NO_2)_2C_6H_3NN{=}CR_1R_2$ (R_1=H for aldehydes). The report described the measurement of carbonyl compounds at the levels of 0.014–0.015 ppb in urban air and the identification of carbonyls at ppb concentrations as reaction products in laboratory studies of the atmospheric oxidation of unsaturated organic compounds.

Let us briefly mention some more details about the application of the ESI method for analyses and identification of FA and their simple derivatives.

LC/ESI-MS Methods for FA Analysis

Low-energy negative-ion ESI-MS and ESI-MS/MS were used (25) to characterize saturated and unsaturated FA. The carbon number and degree of unsaturation of FA were determined. ESI-MS/MS was used to localize double-bond positions of mono- and polyunsaturated FA. For compounds with up to two unsaturated bonds, fragmentation was dominated by the loss of H_2O from the carboxyl moiety and very low-intensity peaks were generated from bonds cleaved at carbons α or β to sites of unsaturation. There was extensive hydride migration during ESI-MS/MS of compounds with three or more double bonds and the localization of double and triple bonds was very difficult. Detection limits for negative-ion ESI-MS/MS were at or below 1 pg.

Features of MS-MS of dilithiated adduct ions of unsaturated FA, obtained by ESI-MS with low-energy collisionally activated dissociation on a triple-stage quadrupole instrument, were described (26). These spectra distinguished among isomeric unsaturated FA and permitted the assignment of double-bond location. The spectra contained radical cations reflecting cleavage of bonds between the first and second and between the second and third carbon atoms in the FA chain. These ions were followed by a closed-shell ion series with members separated by 14 units that reflected cleavage of bonds between the third and fourth and then between subsequent adjacent pairs of carbon atoms.

The use of EI and ESI for the determination of branching positions and localization of unsaturation in FA was described in a report by Vetter and colleagues (27). A new derivative of the carboxyl group, *N*-methyl-2-alkylimidazoline (MIM), was introduced with the aim of improving the control of FA fragmentation. The results obtained from saturated chains were very similar to those generated by EI. The current data do not permit us to formulate definitive rules for the fragmentation of the MIM derivatives of PUFA.

LC/ESI-MS of Dimethylaminoethyl and Trimethylaminoethyl Esters

The development of a new derivative, the dimethylaminoethyl ester (DMAE), for the analysis of FA by ESI-MS/MS was described by Johnson (28). Qualitative and quantitative analyses of long-chain to VLCFA in plasma, blood, urine, and wax were performed. Branched chain, unsaturated, dicarboxylic, hydroxy, amino, and oxo acids were also studied.

The mass spectrum of the DMAE ester of arachidic acid was dominated by an $[M+H]^+$ at *m/z* 384. It yielded strong product ions at *m/z* 339, 90, and 72. The ion at *m/z* 90 was identified as protonated dimethylaminoethanol that had been eliminated from the DMAE ester. The ion at *m/z* 72 is probably an immonium ion, $MeHC{=}N^+Me_2$, commonly generated from aliphatic amines.

Further, the trimethylaminoethyl (TMAE) ester iodide (29) affords between 8 and 12 times greater signal intensity than the corresponding dimethylaminoethyl ester used in the analysis of long-chain to VLCFA. It is a superior derivative for unsaturated and monohydroxylated long-chain FAs but was unsuitable for bile acids and dicarboxylic acids. The product ion spectra of the molecular cations of all TMAE derivatives of saturated FA from acetic to triacontanoic contained a $[M–C_3H_9N]^+$ ion as the most intense ion. As observed for DMAE esters, there was no difference in the mass spectra or product ion spectra of derivatives of straight-chain and multiple-branched FA of the same molecular mass.

In contrast to DMAE esters, the molecular cations of TMAE derivatives of unsaturated FA yielded $[M–C_3H_9N]^+$ product ions of similar intensity to those obtained from saturated FA with the same number of carbon atoms. Unlike GC-MS, which separates isomeric forms, the PUFA identified by ESI-MS/MS represent the total of all of the ω-3, ω-6, ω-9, and so on, series isomers.

An obvious shortcoming of the ESI-MS/MS method used for analyzing hydroxy FA is that all the isomeric forms such as 2-, 3-, and ω-hydroxy isomers are measured collectively.

LC/ESI-MS of Oxidized FA

Negative-ion ESI-MS and ESI-MS/MS were used to characterize saturated and unsaturated monohydroxy FA and FA metabolites formed by incubation with soybean lipoxygenase (30). Ions corresponding to the $[M–H]^–$ of eicosanoids were readily observed by using ESI-MS, but double-bond migration precluded the use of MS to localize double bonds or the position of hydroxyl moieties; however, by following MS analysis with negative-ion ESI-MS/MS of precursor ions, the position of oxygenation could be determined for picogram quantities of underivatized monohydroxy FA.

Two reports (31,32) describing ESI and low-energy MS-MS of polyhydroxy unsaturated FA and negative-ion ESI-MS/MS structural characterization of leukotriene B_4-derived metabolites were published. The low-energy collision-induced dissociation (CID) of the carboxylate anions generated by ESI of leukotriene B_4 and 16 of its metabolites was studied in a tandem quadrupole mass spectrometer (31).

Negative ESI, fast atom bombardment (FAB), and low-energy MS-MS were used for the analysis of dihydroxyeicosatrienoic acids containing a vicinal diol and three nonconjugated double bonds, of dihydroxyeicosatetraenoic acids, which contain a conjugated triene structure, and of trihydroxyeicosatetraenoic acids, which contain a vicinal diol and a conjugated tetraene structure (32).

A rapid method was described for the identification of FA hydroperoxides by LC/ESI-MS/MS without any derivatization required before analysis (33).

A new interface for capillary electrophoresis (CE-ESI) was presented (34). The liner has been evaluated for the analysis of FA and prostaglandins, all run with negative ESI.

Direct analysis (35) of intact long-chain fatty acyl CoA esters was investigated by using matrix-assisted laser desorption time-of-flight MS and ESI-MS. Decomposition of the $[M+H]^+$ ion of hexadecyl coenzyme A at *m/z* 1006 yielded a prominent product ion at *m/z* 499 characteristic for the fatty acyl portion of the molecule. Similar fatty acyl product ion fragments, corresponding to a neutral loss of *m/z* 609, were found for the $[M+H]^+$ species of all of the fatty acyl CoA esters investigated.

Acylcarnitines were used for determining the β-oxidation defects in patients (neonatal and prenatal inborn errors) with biochemically heterogeneous diseases (see Table 5.5) (36–49). This method was also used for detection of further metabolic disorders (50–52). Also, the structures of lipid A and further bacterial lipids were determined by ESI-MS methods (53–57).

ESI-MS/MS analyses were performed on phospholipid and cholesterol esters without any previous chromatographic separation (58). The fragmentation of cholesterol esters was shown and a fragment ion at *m/z* 369 was the most abundant product ion of cholesterol esters.

The study by Kerwin and colleagues (59) described the use of positive- and negative-ion ESI with MS-MS to identify glycerophospholipid and ceramide headgroups and their alkyl, alkenyl, and acyl constituents.

Conclusions

The largely unsatisfactory state of the art in APCI of simple derivatives of FA can be summarized as follows:

Fundamental studies that would contain essential details describing the effect of external parameters such as capillary voltage setting, corona current, nebulizer pressure, drying gas flow and temperature, vaporizer temperature, fragmenter settings, and so on, on FA identification have not yet been published. For instance, contradictory data exist on the addition of mobile-phase components (i.e., acetonitrile) to double bond(s) of unsaturated FA. Some authors have identified an ion at $[M+42]^+$, others have found an ion adduct at $[M+54]^+$, and still others did not detect any adduct ions. However, it is commonly known that ions of all types arise during chemical ionization (60). Therefore, all of the possibilities have been considered. For full identification of FA, it is necessary to know the value of the molecular mass, from

TABLE 5.5
Quantitative Plasma Acylcarnitine Analysis Using Electrospray Tandem Mass Spectrometry for the Diagnosis of Organic Acidemias and Fatty Acid Oxidation Defects

Disorder	Diagnostic *m/z* ratio	Acylcarnitines[a]	Reference controls (95th centile[b]), μmol/L	Patients (range[d]), μmol/L
SCAD/EMA	288/274	C_4/C_3	0.98[c]	0.71–9.0[c]
	288/347	C_4/C_8-d_3	0.32	0.80–5.00
	302/274	C_5/C_3	0.80[c]	0.19–4.52[c]
	302/347	C_5/C_8-d_3	0.22	0.16–0.64
MCAD	316/347	C_6/C_8-d_3	0.12	0.12–2.14
	344/347	C_8/C_8-d_3	0.22	1.16–25.78
	370/347	$C_{10:1}/C_8$-d_3	0.22	0.26–2.24
LCHAD/MTP	472/459	$C_{16}OH/C_{16}$-d_3	0.02	0.12–0.60
	498/459	$C_{18:1}OH/C_{16}$-d_3	0.01	0.14–0.86
	500/459	$C_{18}OH/C_{16}$-d_3	0.04	0.12–0.78
VLCAD	426/459	$C_{14:1}/C_{16}$-d_3	0.18	0.76–13.28
	424/459	$C_{14:2}/C_{16}$-d_3	0.08	0.30–3.48
CPT II	456/459	C_{16}/C_{16}-d_3	0.24	2.06–3.94
	454/459	$C_{16:1}/C16$-d_3	0.08	0.50–0.86
	484/459	C_{18}/C_{16}-d_3	0.10	0.64–1.44
	482/459	$C_{18:1}/C_{16}$-d_3	0.28	1.56–4.32
	480/459	$C_{18:2}/C_{16}$-d_3	0.18	0.54–1.66
GA I	388/347	Glutaryl/C_8-d_3	0.06	0.46–1.34
GA II/MAD	288/274	C_4/C_3	0.98c	2.09–12.54[c]
	302/274	C_5/C_3	0.80c	1.82–6.27[c]
	316/347	C_6/C_8-d_3	0.12	0.22–3.54
	344/347	C_8/C_8-d_3	0.22	0.80–7.96
	372/347	C_{10}/C_8-d_3	0.30	0.82–5.88
HMG-CoA-lyase	318/347	Hydroxy-C_5/C_8-d_3	0.06	0.08–1.42
	402/347	Methylglutaryl/C8-d_3	0.02	0.08–0.70
β-Ketothiolase	300/347	$C_{5:1}/C_8$-d_3	0.04	0.14–0.72
	318/347	Hydroxy-C_5/C_8-d_3	0.06	0.12–0.30
PA	274/263	C_3/C_2-d_3	1.30	6.50–60.10
MMA	274/263	C_3/C_2-d_3	1.30	13.00–70.50
	374/347	Methylmalonyl/C8-d_3	0.06	0.12–0.94
IVA	302/274	C_5/C_3	0.80[c]	52.96–60.47[c]
	302/347	C_5/C_8-d_3	0.22	15.52–18.38

[a]d_3 depicts a labeled internal standard.
[b]The 95th centile of the reference range.
[c]Expressed as ratio.
[d]Range of values found in patient samples, not all concentrations and/or ratios were abnormal in each case.
Abbreviations: SCAD, short-chain acyl-CoA dehydrogenase; MCAD, medium-chain acyl-CoA dehydrogenase; LCHAD/MTP, long-chain 3-hydroxyacyl-CoA dehydrogenase/mitochondrial trifunctional protein; VLCAD, very-long-chain acyl-CoA dehydrogenase; CPT II, carnitine palmitoyltransferase II; GA I, glutaric acidemia type I; GA II/MAD, glutaric acidemia type II/multiple acyl-CoA dehydrogenase; HMG-CoA lyase, 3-hydroxy-3-methylglutaryl-CoA dehydrogenase; BKT, β-ketothiolase; PA, propionic acidemia; MMA, methylmalonic acidemia; IVA, isovaleric acidemia.

which the chain length and number of double bonds can be deduced. However, some samples of natural origin can contain 27:1 and 28:8 FA. Although both FA have the same molecular mass, there are no problems in separating them by chromatography (16).

Unfortunately, the APCI-MS method failed in the identification of the position and configuration of double bonds (*E*/*Z*), as discussed herein for the case of acetonitrile addition to the C=C bond. In particular, the method fails in identification of branched (and polybranched) FA and for FA in which the main chain was substituted by a hydroxyl group or oxygen atom. One report that confirmed the feasibility of the ACPI method in this field was published earlier (8).

As follows from the survey of these reports, APCI methods were applied first in cases of FA identification where classical GC-MS techniques failed. The methods provided unsatisfactory results in the identification of VLCFA and VLCPUFA in natural samples, especially those of exotic origin. As shown herein, the higher fixed and variable costs of analysis by APCI-MS methods must be considered.

Currently, the possibilities of APCI-MS methods are not fully exploited, especially in analysis of simple derivatives of FA. The technique is relatively new and is still waiting for its boom. Because of the commercial availability of LC/APCI-MS systems we would expect an increase of sophisticated APCI applications in LC-MS in the coming years. Unfortunately, the high purchase price and operating costs seem to be the main limitations in the use of LC/APCI-MS. However, the robustness and sensitivity of analyses, the possibility of simultaneous evaluation of the content of chemical compounds, estimation of their chemical structures, and determination of molecular masses all combine to make it a technique of extraordinary value.

References

1. Murphy, R.C., J. Fiedler, and J. Hevko, Analysis of Nonvolatile Lipids by Mass Spectrometry, *Chem. Rev. 101:* 479–526 (2001).
2. Rezanka, T., and V.M. Dembitsky, Very Long Chain Polyunsaturated Fatty Acids in Crustacea of the Order Bathynellacea, *Biochem. Syst. Ecol. 27:* 551–558 (1999).
3. Rezanka, T., Analysis of Polyunsaturated Fatty Acids Using High Performance Liquid Chromatography—Atmospheric Pressure Chemical Ionization Mass Spectrometry, *J. High Resol. Chromatogr. 23:* 338–342 (2000).
4. Sjoberg, P.J.R., and K.E. Markides, Capillary Column Supercritical Fluid Chromatography—Atmospheric Pressure Ionisation Mass Spectrometry-Interface Performance of Atmospheric Pressure Chemical Ionisation and Electrospray Ionization, *J. Chromatogr. A 855:* 317–327 (1999).
5. Banni, S., B.W. Day, R.W. Evans, F.P. Corongui, and B. Lombardi, Liquid Chromatographic-Mass Spectrometric Analysis of Conjugated Diene Fatty Acids in a Partially Hydrogenated Fat, *J. Am. Oil Chem. Soc. 71:* 1321–1325 (1994).
6. Rezanka, T., Analysis of Very Long Chain Polyunsaturated Fatty Acids Using High-Performance Liquid Chromatography—Atmospheric Pressure Chemical Ionization Mass Spectrometry, *Biochem. Syst. Ecol. 28:* 847–856 (2000).

7. Rezanka, T., and V.M. Dembitsky, Tetratriacontanonaenoic Acid, First Natural Acid with Nine Double Bonds Isolated from a Crustacean *Bathynella natans*, *Tetrahedron 60:* 4261–4264 (2004).
8. Rezanka, T., Identification of Very Long Chain Fatty Acids by Atmospheric Pressure Chemical Ionization Liquid Chromatography-Mass Spectroscopy from Green Alga *Chlorella kessleri*, *J. Sep. Sci. 25:* 1332–1336 (2002).
9. Holcapek, M., P. Jandera, and J. Fischer, Analysis of Acylglycerols and Methyl Esters of Fatty Acids in Vegetable Oils and in Biodiesel, *Crit. Rev. Anal. Chem. 31:* 53–56 (2001).
10. Rigol, A., A. Latorre, S. Lacorte, and D. Barcelo, Direct Determination of Resin and Fatty Acids in Process Waters of Paper Industries by Liquid Chromatography/Mass Spectrometry, *J. Mass Spectrom. 38:* 417–426 (2003).
11. Latorre, A., A. Rigol, S. Lacorte, and D. Barcelo, Comparison of Gas Chromatography-Mass Spectrometry and Liquid Chromatography-Mass Spectrometry for the Determination of Fatty and Resin Acids in Paper Mill Process Waters, *J. Chromatogr. A 991:* 205–215 (2003).
12. Piazza, G.J., A. Nunez, and T.A. Foglia, Epoxidation of Fatty Acids, Fatty Methyl Esters, and Alkenes by Immobilized Oat Seed Peroxygenase, *J. Mol. Catal. B Enzymol. 21:* 143–151 (2003).
13. Adas, F., D. Picart, F. Berthou, B. Simon, and Y. Amet, Liquid Chromatography–Mass Spectrometry and Gas Chromatography–Mass Spectrometry of ω- and (ω-1)-Hydroxylated Metabolites of Elaidic and Oleic Acids in Human and Rat Liver Microsomes, *J. Chromatogr. B 714:* 133–144 (1998).
14. Ikeda, M., and T. Kusaka, Liquid Chromatography-Mass Spectrometry of Hydroxy and Non-Hydroxy Fatty Acids as Amide Derivatives, *J. Chromatogr. 575:* 197–205 (1992).
15. Koga, D., T. Santa, T. Fukushima, H. Homma, and K. Imai, Liquid Chromatographic-Atmospheric Pressure Chemical Ionization Mass Spectrometric Determination of Anandamide and Its Analogs in Rat Brain and Peripheral Tissues, *J. Chromatogr. B 690:* 7–13 (1997).
16. Nichols, D.S., and N.W. Davies, Improved Detection of Polyunsaturated Fatty Acids as Phenacyl Esters Using Liquid Chromatography-Ion Trap Mass Spectrometry, *J. Microbiol. Methods 50:* 103–113 (2002).
17. Kusaka, T., and M. Ikeda, LC-MS of Fatty Acids Including Hydroxy and Hydroperoxy Acids as Their 3-Methyl-7-methoxy-1,4-benzoxazin-2-one Derivatives, *J. Chromatogr. 639:* 165–173 (1993).
18. Calaf, R.E., J. Pena, S. Paytubi, M. Carrascal, M. Posada, and E. Gelpi, Automated Strong Cation Exchange Extraction of Fatty Acid Esters of 3-(*N*-Phenylamino)-1,2-propanediol from Oil Samples for Routine Quantification by HPLC-APCI/MS/MS, *J. Agr. Food Chem. 49:* 5085–5091 (2001).
19. Karlsson, A.A., P. Michelsen, and G. Odham, Molecular Species of Sphingomyelin: Determination by High-Performance Liquid Chromatography Mass Spectrometry with Electrospray and High-Performance Liquid Chromatography Tandem Mass Spectrometry with Atmospheric Pressure Chemical Ionization, *J. Mass Spectrom. 33:* 1192–1198 (1998).
20. Kimpe, K., P.A. Jacobs, and M. Waelkens, Mass Spectrometric Methods Prove the Use of Beeswax and Ruminant Fat in Late Roman Cooking Pots, *J. Chromatogr. A 968:* 151–160 (2002).

21. Mitamura, K., Y. Nambu, M. Tanaka, A. Kawanishi, J. Kitahori, and K. Shimada, High-Performance Liquid Chromatographic Separation of Vitamin D-3 3-Fatty Acid Esters and Their Liquid Chromatography Mass Spectrometry, *J. Liq. Chromatogr. Rel. Technol. 22:* 367–377 (1999).
22. Shimada, K., Y. Mukai, A. Nakajima, and Y. Naka, Studies on Neurosteroids, 6: Characterization of Fatty Acid Esters of Pregnenolone and Dehydroepiandrosterone in Rat Brains Using Liquid Chromatography Mass Spectrometry, *Anal. Commun. 34:* 145–146 (1997).
23. Rezanka, T., and V.M. Dembitsky, Identification of Acylated Xanthone Glycosides by Liquid Chromatography–Atmospheric Pressure Chemical Ionization Mass Spectrometry in Positive and Negative Modes from the Lichen *Umbilicaria proboscidea*, *J. Chromatogr. A 995(1-2):* 109–118 (2003).
24. Grosjean, E., P.G. Green, and D. Grosjean, Liquid Chromatography Analysis of Carbonyl (2,4-Dinitrophenyl)hydrazones with Detection by Diode Array Ultraviolet Spectroscopy and by Atmospheric Pressure Negative Chemical Ionization Mass Spectrometry, *Anal. Chem. 7:* 1851–1861 (1999).
25. Kerwin, J.L., A.L. Wiens, and L.H. Ericsson, Identification of Fatty Acids by Electrospray Mass Spectrometry and Tandem Mass Spectrometry, *J. Mass Spectrom. 31:* 184–192 (1996).
26. Hsu, F.F., and J. Turk, Distinction Among Isomeric Unsaturated Fatty Acids as Lithiated Adducts by Electrospray Ionization Mass Spectrometry Using Low Energy Collisionally Activated Dissociation on a Triple Stage Quadrupole Instrument, *J. Am. Soc. Mass Spectrom. 10:* 600–612 (1999).
27. Vetter, W., W. Meister, and G. Oesterhelt, 2-Alkylimidazoline Derivative to Control Fatty Acid Fragmentation upon Electron Impact and Electrospray Ionization, *J. Mass Spectrom. 33:* 461–472 (1998).
28. Johnson, D.W., Dimethylaminoethyl Esters for Trace, Rapid Analysis of Fatty Acids by Electrospray Tandem Mass Spectrometry, *Rapid Commun. Mass Spectrom. 13:* 2388–2393 (1999).
29. Johnson, D.W., Alkyldimethylaminoethyl Ester Iodides for Improved Analysis of Fatty Acids by Electrospray Ionization Tandem Mass Spectrometry, *Rapid Commun. Mass Spectrom. 14:* 2019–2024 (2000).
30. Kerwin, J.L., and J.J. Torvik, Identification of Monohydroxy Fatty Acids by Electrospray-Mass Spectrometry and Tandem-Mass Spectrometry, *Anal. Biochem. 237:* 56–64 (1996).
31. Wheelan, P., J.A. Zirrollia, and R.C. Murphya, Negative Ion Electrospray Tandem Mass Spectrometric Structural Characterization of Leukotriene B4 (LTB4) and LTB4-Derived Metabolites, *J. Am. Soc. Mass Spectrom. 7:* 129–139 (1996).
32. Wheelan, P., J.A. Zirrolli, and R.C. Murphy, Electrospray Ionization and Low-Energy Tandem Mass Spectrometry of Polyhydroxy Unsaturated Fatty Acids, *J. Am. Soc. Mass Spectrom. 7:* 140–149 (1996).
33. Schneider, C., P. Schreier, and M. Herderich, Analysis of Lipoxygenase-Derived Fatty Acid Hydroperoxides by Electrospray Ionization Tandem Mass Spectrometry, *Lipids 32:* 331–336 (1997).
34. Petersson, M.A., G. Hulthe, and E. Fogelqvist, New Sheathless Interface for Coupling Capillary Electrophoresis to Electrospray Mass Spectrometry Evaluated by the Analysis of Fatty Acids and Prostaglandins, *J. Chromatogr. A 854:* 141–154 (1999).

35. Hankin, J.A., and R.C. Murphy, MALDI-TOF and Electrospray Tandem Mass Spectrometric Analysis of Fatty Acyl-CoA Esters, *Int. J. Mass Spectrom. Ion Processes 165:* 467–474 (1997).
36. Chace, D.H., S.L. Hillman, J.L. Van Hove, and E.W. Naylor, Rapid Diagnosis of MCAD Deficiency: Quantitative Analysis of Octanoylcarnitine and Other Acylcarnitines in Newborn Blood Spots by Tandem Mass Spectrometry, *Clin. Chem. 43:* 2106–2113 (1997).
37. Millington, D.S., N. Kodo, D.L. Norwood, and C.R. Roe, Tandem Mass Spectrometry: A New Method for Acylcarnitine Profiling with Potential for Neonatal Screening for Inborn Errors of Metabolism, *J. Inherit. Metab. Dis. 13:* 321–324 (1990).
38. Nada, M.A., C. Vianey-Saban, and C.R. Roe, Prenatal Diagnosis of Mitochondrial Fatty Acid Oxidation Defects, *Prenat. Diagn. 16:* 117–124 (1996).
39. Rashed, M.S., P.T. Luand, M.P. Bucknall, and D. Little, Diagnosis of Inborn Errors of Metabolism from Blood Spots by Acylcarnitines and Amino Acids Profiling Using Automated Electrospray Tandem Mass Spectrometry, *Pediatr. Res. 38:* 324–331 (1995).
40. Rashed, M.S., P.T. Luand, M.J. Bennett, J.J. Barnard, D.R. Govindaraju, and P. Rinaldo, Inborn Errors of Metabolism Diagnosed in Sudden Death Cases by Acylcarnitine Analysis of Postmortem Bile, *Clin. Chem. 41:* 1109–1114 (1995).
41. Rashed, M.S., M.P. Bucknall, and D. Little, Screening Blood Spots for Inborn Errors of Metabolism by Electrospray Tandem Mass Spectrometry with a Microplate Batch Process and a Computer Algorithm for Automated Flagging of Abnormal Profiles, *Clin. Chem. 43:* 1129–1141 (1997).
42. Shigematsu, Y., I. Hata, and A. Nakai, Prenatal Diagnosis of Organic Acidemias Based on Amniotic Fluid Levels of Acylcarnitines, *Pediatr. Res. 39:* 680–684 (1996).
43. Van Hove, J.L., W. Zhang, and S.G. Kahler, Medium-Chain Acyl-CoA Dehydrogenase (MCAD) Deficiency: Diagnosis by Acylcarnitine Analysis in Blood, *Am. J. Hum. Genet. 52:* 958–966 (1993).
44. Van Hove, J.L., S.L. Rutledge, M.A. Nada, S.G. Kahler, and D.S. Millington, 3-Hydroxyisovalerylcarnitine in 3-Methylcrotonyl-CoA Carboxylase Deficiency, *J. Inherit. Metab. Dis. 18:* 592–601 (1995).
45. Vreken, P., A.E.M. van Lint, A.H. Bootsma, H. Overmars, R.J.A. Wanders, and A.H. Van Gennip, Quantitative Plasma Acylcarnitine Analysis Using Electrospray Tandem Mass Spectrometry for the Diagnosis of Organic Acidaemias and Fatty Acid Oxidation Defects, *J. Inherit. Metab. Dis. 22:* 302–306 (1999).
46. Giak Sim, K., K. Carpenter, J. Hammond, J. Christodoulou, and B. Wilckena, Quantitative Fibroblast Acylcarnitine Profiles in Mitochondrial Fatty Acid β-Oxidation Defects: Phenotype/Metabolite Correlations, *Mol. Genet. Metab. 76:* 327–334 (2002).
47. Ford, D.A., X.L. Han, C.C. Horner, and R.W. Gross, Accumulation of Unsaturated Acylcarnitine Molecular Species During Acute Myocardial Ischemia: Metabolic Compartmentalization of Products of Fatty Acyl Chain Elongation in the Acylcarnitine Pool, *Biochemistry 35:* 7903–7909 (1996).
48. Vreken, P., A.E.M. van Lint, A.H. Bootsma, H. Overmars, R.J.A. Wanders, and A.H. van Gennip, Rapid Diagnosis of Organic Acidemias and Fatty-Acid Oxidation Defects by Quantitative Electrospray Tandem-MS Acyl-Carnitine Analysis in Plasma, *Adv. Exp. Med. Biol. 466:* 327–337 (1999).
49. Sim, K.G., K. Carpenter, J. Hammond, J. Christodoulou, and B. Wilcken, Quantitative Fibroblast Acylcarnitine Profiles in Mitochondrial Fatty Acid β-Oxidation Defects: Phenotype/Metabolite Correlations, *Mol. Genet. Metab. 76:* 327–334 (2002).

50. Hsu, F.F., A. Bohrer, M. Wohltmann, S. Ramanadham, Z.M. Ma, K. Yarasheski, *et al.*, Electrospray Ionization Mass Spectrometric Analyses of Changes in Tissue Phospholipid Molecular Species During the Evolution of Hyperlipidemia and Hyperglycemia in Zucker Diabetic Fatty Rats, *Lipids 35:* 839–854 (2000).
51. Murthy, M., J. Hamilton, R.S. Greiner, T. Moriguchi, N. Salem, and H.Y. Kim, Differential Effects of n-3 Fatty Acid Deficiency on Phospholipid Molecular Species Composition in the Rat Hippocampus, *J. Lipid Res. 43:* 611–617 (2002).
52. Johnson, D.W., and M.U. Trinh, Analysis of Isomeric Long-Chain Hydroxy Fatty Acids by Tandem Mass Spectrometry: Application to the Diagnosis of Long-Chain 3-Hydroxyacyl CoA Dehydrogenase Deficiency, *Rapid Commun. Mass Spectrom. 17:* 171–175 (2003).
53. Corsaro, M.M., F.D. Piaz, R. Lanzetta, and M. Parrilli, Lipid A Structure of *Pseudoalteromonas haloplanktis* TAC 125: Use of Electrospray Ionization Tandem Mass Spectrometry for the Determination of Fatty Acid Distribution, *J. Mass Spectrom. 37:* 481–488 (2002).
54. Kussak, A., and A. Weintraub, Quadrupole Ion-Trap Mass Spectrometry to Locate Fatty Acids on Lipid A from Gram-Negative Bacteria, *Anal. Biochem. 307:* 131–137 (2002).
55. Vanderdrift, K.M.G.M., H.P. Spaink, G.V. Bloemberg, A.A.N. Van Brussel, B.J.J. Lugtenberg, J. Haverkamp, *et al.*, *Rhizobium leguminosarum* bv. *trifolii* Produces Lipo-Chitin Oligosaccharides with Node-Dependent Highly Unsaturated Fatty Acyl Moieties: An Electrospray-Ionization and Collision-Induced Dissociation Tandem-Mass Spectrometric Study, *J. Biol. Chem. 271:* 22563–22569 (1996).
56. Rutters, H., H. Sass, H. Cypionka, and J. Rullkotter, Microbial Communities in a Wadden Sea Sediment Core—Clues from Analyses of Intact Glyceride Lipids, and Released Fatty Acids, *Org. Geochem. 33:* 803–816 (2002).
57. Toledo, M.S., S.B. Levery, E. Suzuki, A.H. Straus, and H.K. Takahashi, Characterization of Cerebrosides from the Thermally Dimorphic Mycopathogen *Histoplasma capsulatum*: Expression of 2-Hydroxy Fatty *N*-Acyl (*E*)-δ-3-Unsaturation Correlates with the Yeast-Mycelium Phase Transition, *Glycobiology 11:* 113–124 (2001).
58. Duffin, K., M. Obukowicz, A. Raz, and J.J. Shieh, Electrospray/Tandem Mass Spectrometry for Quantitative Analysis of Lipid Remodeling in Essential Fatty Acid Deficient Mice, *Anal. Biochem. 279:* 179–188 (2000).
59. Kerwin, J.L., A.R. Tuininga, and L.H. Ericsson, Identification of Molecular Species of Glycerophospholipids and Sphingomyelin Using Electrospray MS, *J. Lipid Res. 35:* 1102–1114 (1994).
60. Moneti, G., G. Pieraccini, F. Dani, S. Turillazzi, D. Favretto, and P. Traldi, Ion-Molecule Reactions of Ionic Species from Acetonitrile with Unsaturated Hydrocarbons for the Identification of the Double-Bond Position Using an Ion Trap, *J. Mass Spectrom. 32:* 1371–1373 (1997).